Utrecht University

Kinetics Study of a Pd-catalyzed Hydrogenation Reaction

Studied with Fluorescence Spectroscopy

Bryan Folmer

Daily Supervisor: MSc. Stijn Hinterding

Bachelor's Thesis in Chemistry
Inorganic Chemistry and Catalysis
Soft Condensed Matter

3rd July 2019

Examination:

MSc. Stijn Hinterding

Dr. Freddy Rabouw

ABSTRACT

In this research, reaction kinetics of a Pd-catalyzed hydrogenation reaction are studied. One particular boron-dipyrromethene molecule was hydrogenated. Research goals are how differently shaped nanoparticles, cubic and cuboctahedral shaped, affected the catalytic activity, how the concentrations of both reactant and hydrogen donor affect the rate constant of this particular reaction. Therefore, experiments for different concentrations of these parameters are performed. Results show that the Pd-catalyzed hydrogenation reaction follows the Langmuir-Hinshelwood mechanism and has increasing rate constants for higher concentrations of hydrogen. The Bodipy-dye stock solution contains an inhibitor for the hydrogenation reaction, with increasing rate constants at lower concentrations. At last, nanoparticles enclosed by {100} and {111} facets show more catalytic activity than nanoparticles enclosed by {100} facets only.

Table of Contents

1: Introduction

In the recent years, interest in catalytic hydrogenation has risen in most fields of chemistry. Hydrogenation is defined as adding molecular hydrogen to unsaturated compounds, such as alkenes or alkynes. This phenomenom has been studied since 1897, when catalytic hydrogenation was discovered (1). In most cases, hydrogenation is only successful in the presence of a catalyst. Intensive research has been carried out for years, because catalytic hydrogenation is used extensively in industrial applications. These applications range from petrochemical to nutritional purposes. In oil refineries, more than 31 billion barrels of crude oil are processed, which is in conjugation with a value of over 3 billion on platinum catalysts needed for this process (2).

Due to this large scale, the urge of gaining more knowlegde and understanding about the mechanism and kinetics of catalytic hydrogenation is extremely important. Hydrogenation involves both kinetics and thermodynamics. However, the presence of a metal catalysts can only influence kinetics, and does not affect thermodynamics. Several reaction models are formulated and provide an explanation for the function of metal catalysts. In addition, properties of the catalysts have been thoroughly investigated. Different elements, geometry and size are known to affect the catalytic performance (3).

However, there is lack of knowledge on the behavior of molecules on a single-molecular scale. In order to be able to investigate the single-molecular behavior, suitable conditions must be found. These conditions, kinetics and behavior of this reaction and molecules can more easily be investigated on bulk scale, because analytical methods are applied more easily and cost less time.

This research focusses on studying the kinetics of Palladium-catalyzed hydrogenation of boron-dipyrromethene-dimethyl-styryl on a larger scale. This reactant is a derivate of the Bodipy family and is abbreviated as Bodipy-DMS. These dyes possess fluorescent properties, and these properties are needed for single-molecule analysis. Kinetics of the reaction will be analyzed for multiple reaction conditions. Results of this bulk research project provide useful information for future measurements on a single-molecule scale.

2: Methodology.

The information in this chapter explains the approach for achieving the research goals and provides answers. First of all, the overall research is explained and backed up by theory. Secondly, the experimental approach of this research is described. The experimental part will contain procedures and multiple observations acquired during practical work.

2.1 Goal of the research.

The goal of this particular research is gaining more insight in the Bodipy hydrogenation reaction, which involves both kinetics and the mechanism. A lot of Bodipy dye derivatives are known and can be synthesized, but this research will focus on one Bodipy reactant, which is pre-synthesized by the supervisor and is available.

Main research question:

How is the reaction rate of the Pd-catalyzed hydrogenation of 1,3-dimethyl-5-styryl Bodipy affected by different reactant concentrations and differently shaped metal catalysts?

***Sub-questions**:*

- What kinetics are involved in a Pd-catalyzed hydrogenation reaction?
- What is the effect of the concentration of hydrogen on the reaction rate of Pd-catalyzed hydrogenation?
- How does the concentration of Bodipy-DMS influence the reaction rate?
- How do differently shaped catalytic nanoparticles affect the reaction rate?

2.2 Overview of reaction.

Hydrogenation is defined as adding molecular hydrogen to a functional group, more regularly to alkynes or alkenes, which involves C=C bond. Hydrogenation can also be seen as the hybridization of atomic orbitals, which are sp and sp^2. Adding molecular hydrogen is done in the presence of metal catalysts, for example palladium or platinum.

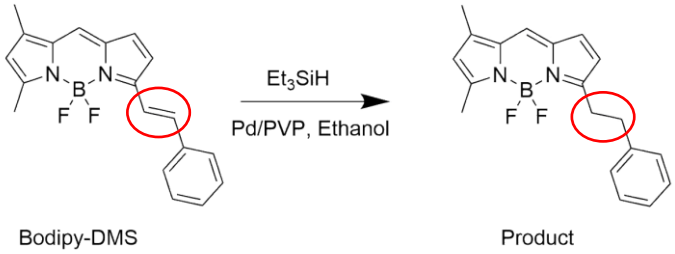

Figure 1: Reaction Model of Hydrogenation.

Figure 1 is the reaction which is studied in this research. The reactant, Bodipy-DMS, possess fluorescent properties. These properties can be used to monitor conversion with fluorescence spectroscopy. This analytical method is relatively simple and involves measuring the fluorescence intensity of a certain sample over time at different wavelengths.

Triethylsilane, abbreviated as Et_3SiH in figure 1, is the supplier of hydrogen during the reaction, in conjunction with ethanol. At last, the metal catalyst will be palladium, stabilized on polyvinylpyrrolidone.

The reactant emits light at 570nm. Once the reaction has started, the reactant will be hydrogenated and the product will be formed. This product shows fluorescence at a different wavelength, at approximately 520 nm. Therefore, a color shift from yellow to green over time can be observed, shown by figure 2.

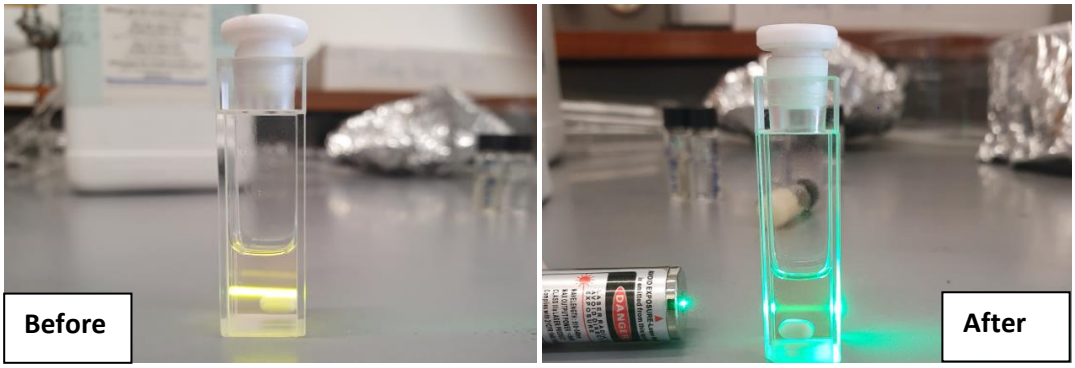

Figure 2: Color difference between reactant and product.

2.3: Theory.

In this chapter, relevant and applied theory to the research will be discussed and explained, from basic to more complex situations.

2.3.1: Fluorescence.

The basics of fluorescence have to be understood in order to be able to acquire data. Fluorescence is known as emission of light by a compound or molecule which has absorbed light in earlier stages, and stops emitting light immediately after the light source is turned off. Molecules and electrons are known to have different energy levels. Most of the time, electrons are occupying the so called 'ground' state, which is defined as the lowest possible energy level. Electrons within a molecule can be excited to higher energy levels by absorbing a photon supplied by a light source. After a nanosecond time period, electrons fall back to their original ground state, shown by figure 3. The transition from higher to lower energy levels, is paired with emission of light with a particular wavelength, which is 570 nm for the reactant and 520nm for the product. These wavelengths are related to the difference in height of the energy levels.

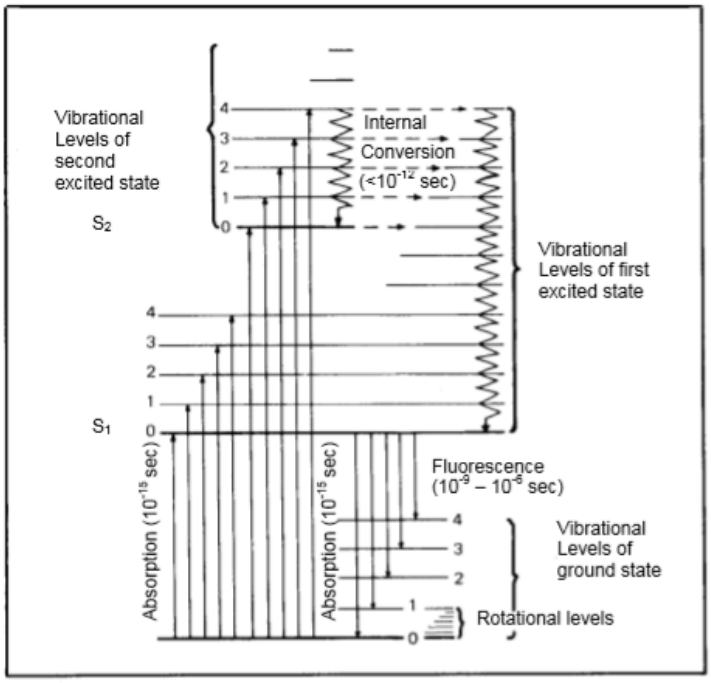

Figure 3: Transition between energy levels, generating absorption and emission (4)

To observe fluorescence, a light source is needed. In this particular situation, a laser is sufficient, which emits monochromatic light at 520nm. A laser will provide the photons needed for exciting electrons to higher energy levels.

In general, different analytical methods can be applied, such as Infrared Spectroscopy. However, the future goal is to analyze on a single-molecular scale. Therefore, fluorescence is preferred over all other analytical methods.

2.3.2: Fluorescence color shift.

The prerequisite for using fluorescence spectroscopy, is that both reactant and product show fluorescence at separate wavelengths. If not, the formation of products and performance of reaction cannot be evaluated. Therefore, the reactant is synthesized specifically for this color shift.

The emission of light at different wavelengths can be explained by the concept of conjugated π-systems. The reactant possesses multiple π-bonds. These C=C bonds are existing of so-called p orbitals. The conjugated system consists of overlapping p-orbitals, which allow π-electrons to delocalize. The delocalization of π-electrons lowers the different energy levels within the molecule, because the delocalization contributes to the stability of the molecule. This stability is the result of the different resonance forms a molecule can form.

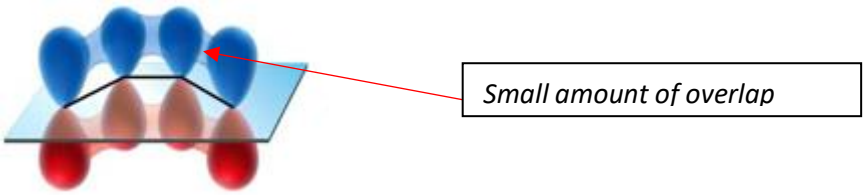

Figure 4: Overlapping π-orbitals *(5).*

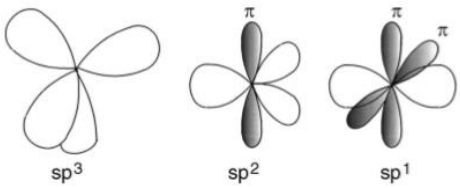

Sp^3 hybridized bonding will occur after hydrogenation.

Figure 5: Hybridized bonding of orbitals (6).

For the product, fluorescence at 520nm is observed. In the product, one specific C=C bond is hydrogenated, which means that the π-bond is replaced by an σ-bond. This reduces the size of conjugated π-system. This reduction of the conjugated π-system leads to the formation of sp^3 bonding, and overlap is not possible anymore, and the conjugated π-system is reduced. This phenomenon destabilizes the molecule, and the energy difference between ground state and excited states increases. This is translated to lower fluorescence wavelength i.e. higher energies.

2.3.3: General concept catalysis.

In general, catalysis deals with lowering the activation energy of the reaction, without catalysts being consumed during the conversion of reactant to product. One of the most important equations in catalysis is the Arrhenius equation, which explains the relation between rate constants and temperature:

$$k = A * e^{-\frac{E_a}{RT}} \text{ [1]}$$

In which k is the rate constant, A is the pre-exponential factor, $\mathrm{E_a}$ is the activation energy, T is the temperature and R is the general gas constant. The activation energy is most important to catalysis, it represents the energy needed for a reaction to occur. Generally, the use of a catalyst for a reaction lowers the activation energy.

Catalysis involves kinetics only, thermodynamics do play a role, but are not affected with the presence of catalysts. The rate of the catalytic hydrogenation reaction can be represented relatively simplistic, shown by equation 2:

$$Rate = k[catalyst][A][B] \text{ [2]}$$

Variable k is the rate constant of the hydrogenation reaction, [A] is the concentration of the Bodipy-DMS and [B] is the concentration of hydrogen.

2.3.4: Mechanism of triethylsilane as hydrogen donor.

To be able to perform hydrogenation, hydrogen must be supplied either by pure molecular hydrogen or by a hydrogen supplying solvent. Based on (7), triethylsilane was chosen to be the supplier of hydrogen, combined with ethanol. This hydrogen donor is used instead of pure molecular hydrogen, because it has multiple advantages. First of all, the use of a hydrogen donor solvent is much more convenient, due to the more complicated setup and needed when using molecular hydrogen. In addition, it makes the system more simple, because both hydrogen donor solvent and your reactant are in the same solvent (8). Secondly, these hydrogen transfer reaction show excellent selectivity and activity (7). Molecular hydrogen can be formed with the help of a Pd-catalysts, according to the following mechanism:

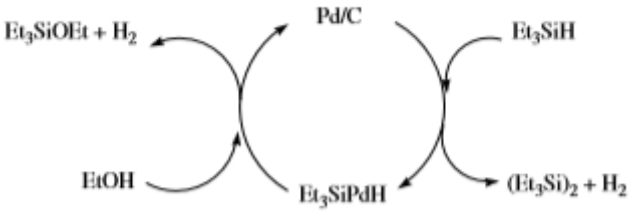

Figure 6: Formation of Molecular Hydrogen by Triethylsilane (7).

$$Et_3SiH + 2^* \leftrightarrow H^* + Et_3Si^* \text{ [3]}$$

$$Et_3Si^* + EtOH + \Theta^* \leftrightarrow Et_3SiOEt + H^* \text{ [4]}$$

In which Et_3SiH represent the hydrogen donor, EtOH is ethanol, * indicates a free site on the catalytic surface and Θ^* represent the fraction of free active sites.

Figure 6 shows that a metal hydride is formed. The metal hydride can either react with ethanol, or with another triethylsilane molecule. In the reaction sample, ethanol is used as a solvent, and is in high amounts of excess present. Therefore, the pathway given by equation 3 and 4 is most likely. Equation 4 represents a reaction step which is very fast, and therefore the rate of this intermediate reaction is mostly determined by equation 3.

2.3.5: Langmuir-Hinshelwood model + kinetics.

Many models have been developed for Pd-catalyzed hydrogenation, but this Pd-catalyzed hydrogenation reaction is assumed to be following the Langmuir-Hinshelwood model (9), for which the concept is shown in figure 7. In this subchapter, multiple kinetic equations will be provided. Catalysis, *Concept and Green applications, Rothenberg* (10) will be used a guideline. Equations are either originating or deviated from this source.

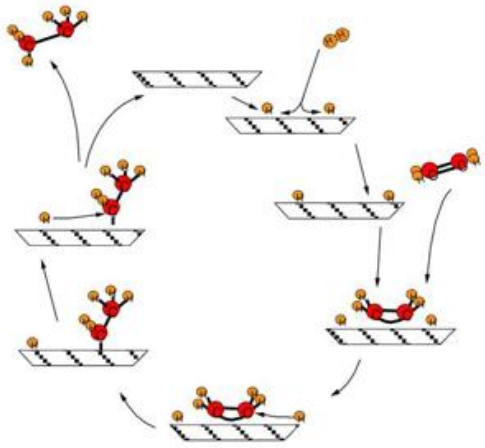

Figure 7: Model of the reaction according to the Langmuir-Hinshelwood model, hydrogenation of ethylene (11).

Figure 7 shows that the reactants are following a route of adsorption, reaction and desorption of the catalyst's surface. First of all, the hydrogen is absorbed on the catalytic surface, then the reactant will absorb on the catalytic surface. Subsequently, it will be hydrogenated within a few steps. The reaction takes place on the active site of the catalyst. The absorption and desorption on an active site is an equilibrium, which is represented by equation 5-7.

$$A + * \leftrightarrow A^* \; [5]$$

$$rate = k_1[A]\Theta^* - K_{-1}\Theta_A \; [6]$$

$$K_A = \frac{\Theta_A}{[A]\Theta_\#} \; [7]$$

Parameter A is defined as Bodipy-DMS, [A] is the concentration of Bodipy-DMS * is adsorption on active site of catalyst, k_1 is the rate constant for adsorption on active site, Θ_A is the fraction active sites occupied by A, $\Theta_\#$ is the fraction of unoccupied active sites, and k_{-1} is the rate constant for desorption on the active sites. The same equation can be formulated for reactant B, which is the hydrogen donor solvent.

Note: The next equations were formulated after results were obtained, so initial expectations were to observe an optimum rate due to competition for active sites.

$$A + * \leftrightarrow A^* [8]$$

$$A^* + H^* \leftrightarrow AH^* + * [9]$$
$$AH^* + H^* \leftrightarrow B + 2^* [10]$$

The * mark indicates absorption/desorption on the catalytic surface. There is an equilibrium which is given by equation 11. For the different reactants, a more specific equilibrium can be formed:

$$K_H = \frac{\Theta_{H*[Et_3SiOEt]}}{[Et_3SiH]*[EtOH]*\Theta^*} [11]$$

$$K_A = \frac{\Theta_A}{[A]*\Theta_\#} [12]$$

$$K_{AH} = \frac{\Theta_{AH}*\Theta^*}{[\Theta_A*\Theta_{Et_3SiH}]} [13]$$

Equation 11 represents the equilibrium constant of K_H, which is the ratio between absorbed hydrogen on the catalytic surface and free hydrogen. This equation is derived from chemical equation 3 and 4. Equation 12 can be derived from equation 8 and Equation 13 can be derived from equations 9 and 10. Both K_A and K_{AH} are equilibrium constants for absorbed/free intermediates. For the formation of the product, equation 10 represent the rate-determining-step. The rate-determining-step is the slowest step within the overall reaction, and directly determines the rate of the reaction. Therefore, the rate of the overall reaction can be formulated as:

$$r = k_{rds} * \Theta_{AH} * \Theta_H [14]$$

Variable k_{RDS} represents the equilibrium of the rate-determining-step, Θ_{AH} the fraction of occupied active sites by AH*, and Θ_H* the fraction of occupied active sites by hydrogen.

A Pd-catalytic nanoparticle adsorbs the reactant on its available active sites. For the total active sites of the catalyst, an equation can be formed relatively:

$$\Theta_{AH} + \Theta_H + \Theta_\# + \Theta_A = 1 [15]$$

In which Θ_{AH}, Θ_H, and Θ_A represent the fraction of active sites occupied by different formed intermediates and $\Theta_\#$ the fraction of free active sites.

By deriving a function for $\Theta_\#$ an overall rate function for the reaction can be formulated, based on the rate-determining-step formula from equation 14:

$$R = \frac{k(K_{AH}(K_H([\frac{[Et_3SiH][EtOH]}{[EtSiOEt]})^2 * K_A[A])}{\left(K_H\left([\frac{[Et_3SiH][EtOH]}{[EtSiOEt]})(1+K_AK_{AH}[A])+K_A[A]\right)\right)^2} [16]$$

2.4: Experimental methods.

First of all, knowledge was acquired by studying multiple papers, which were provided. These papers addressed topics such as hydrogenation and catalysts synthesis. Secondly, once the procedures for catalyst synthesis were formed and approved, the procedures were carried out. The catalysts were functional, which was verified by executing a pilot measurement. Subsequently, parameters were varied and data was analyzed. The analysis of the results was done with Excel and Python. Finally, results were compared with theory and other relevant papers regarding hydrogenation reaction kinetics.

2.4.1: Catalyst Pd-Nanoparticle synthesis.

For the synthesis of the Pd-Nanoparticles, a setup consisting of a heating-plate, oil bath and thermometer was used. The cooling column was excluded, assuming the system was closed and evaporation of reaction mixture could be neglected.

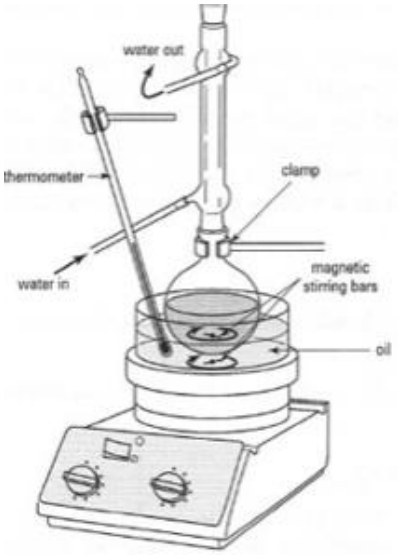

Figure 8: Schematic overview of Catalysts nanoparticle synthesis (12).

In order to be able to start the synthesis, chemicals could be obtained from storage rooms. Cubic Pd-nanoparticles were obtained by heating 11 mL of aqueous solution for 3h at 80℃, which contained a palladium salt, potassium bromide, L-ascorbic acid and polyvinylpyrrolidone. Cuboctahedron Pd-nanoparticles were obtained by heating 11 mL of aqueous solution for 26h at 90℃. This aqueous solution contained a palladium salt, sodium citrate monobasic and polyvinylpyrrolidone.

Both aqueous solution described previously, were prepared based on the same procedures. Appropriate amounts of these chemicals were weighed on an analytical scale and solved. The palladium salt was solved separately. The weighed amounts are shown in table 2. Secondly, the palladium salt solution was sonicated in order to fully solve the palladium salt. Thirdly, the aqueous solution which did not contain the palladium salt was transferred to a round bottom flask and heated to 80℃ or 90℃, depending on which Pd-nanoparticles were synthesized. Finally, the palladium salt solution was added. Once the Pd-precursor solution was added, a color change was noticed. For the cubic Pd-nanoparticles, the reaction mixture was slightly yellow/brown. The cuboctahedron Pd-nanoparticles solution was slightly yellow at the start, but the color developed towards black over time. After 26h, the reaction mixture was black.

Table 1: Function of components in catalyst synthesis**.**

Reaction Mixture	***Chemical***	***Function in Synthesis***
Cubic Pd-NP	*Na_2PdCl_4*	*Provide precursor ions.*
	KBr	*Capping agent.*
	L-ascorbic acid	*Reducing agent.*
	polyvinylpyrrolidone	*Stabilizer*
Cuboctahedron Pd-NP	*Na_2PdCl_4*	*Provides precursor ions.*
	polyvinylpyrrolidone	*Stabilizer.*
	Sodium Citrate monobasic	*Reducing and Capping agent.*

Table 2: Amount of reactants in reaction mixture.

Reaction Mixture	**Chemical**	**Amount solved**	**Amount to heated solution**
Cubic Pd-NP	Na_2PdCl_4	60.3 mg in 3.5mL	3.0 mL
	KBr	312.5 mg in 8mL	-
	L-ascorbic acid	59.1 mg in 8mL	-
	polyvinylpyrrolidone	107.4 mg in 8mL	-
Cuboctahedron Pd-NP	Na_2PdCl_4	27.9 mg in 3.5mL	3.0 mL
	polyvinylpyrrolidone	45.3 mg in 8 mL	-
	Sodium Citrate monobasic	66.2 mg in 8 mL	-

The reaction mixtures were centrifuged and washed.

- Cubic Pd-nanoparticles: centrifuged for 20 minutes at 17000 RCF (5 mL Eppendorf tubes), and washed subsequently with acetone. Supernatant was taken out of Eppendorf tubes, and black solid precipitated. These Pd-nanoparticles were solved in ethanol. The solution was transferred and divided among two 40 mL flask, which means the solution is approximately solved in 70 mL ethanol.
- Cuboctahedron Pd-nanoparticles: centrifuged for 17h at 21000 RCF (2 mL micro centrifuge tubes), not washed once due to centrifugation time. The amount of black solid was little, and the supernatant was taken off. Subsequently, the black solid was solved in ethanol, and transferred to a 40 mL flask. In total, approximately 10 mL of ethanol was used to solve these Pd-nanoparticles.

2.4.2: TEM Image acquirement and analysis.

To acquire TEM-images, one single drop of the synthesized Pd-nanoparticles solved in ethanol, was put on a copper TEM support grid. TEM-images were provided by supervisors certified for the operation of Transmission Electron Microscopes. The TEM-images were analyzed by ImageJ software. The particle size was determined by hand, to ensure accurate results.

2.4.3: Inductively Coupled Plasma Atomic Emission Spectroscopy.

The concentration of the Pd-nanoparticles solved in ethanol was determined by ICP-AES. Samples for these measurements were prepared within a concentration range of 0.1-10ppm. First of all, concentrations of the Pd-nanoparticle solutions were estimated. For the Pd-nanocubes, 100% yield was assumed, solved in 70 mL of ethanol. The synthesis of the cuboctahedron Pd-nanoparticles was assumed to be less successful, and assumed to have approximately 50% yield, solved in 10 mL of ethanol. The difference in yield for both solutions are reasoned by the amount of black solid precipitated after centrifugation.

First of all, different dilutions of the Pd-nanoparticles stock solution were made. Secondly, empty 15 mL vials were weighted. A certain amount of these diluted solutions were added to these vials afterwards. The solvent, ethanol, was evaporated by air. Black solid at the bottom of these vials was observed. Subsequently, nitric acid (20 µL) and hydrochloric acid (60 µL) was added to achieve Aqua regia between 1-5%, which is a requirement for ICP-AES samples. Therefore, 4.9 mL of ethanol was added and the vials were weighted.

2.4.4: Measurement setup + procedure.

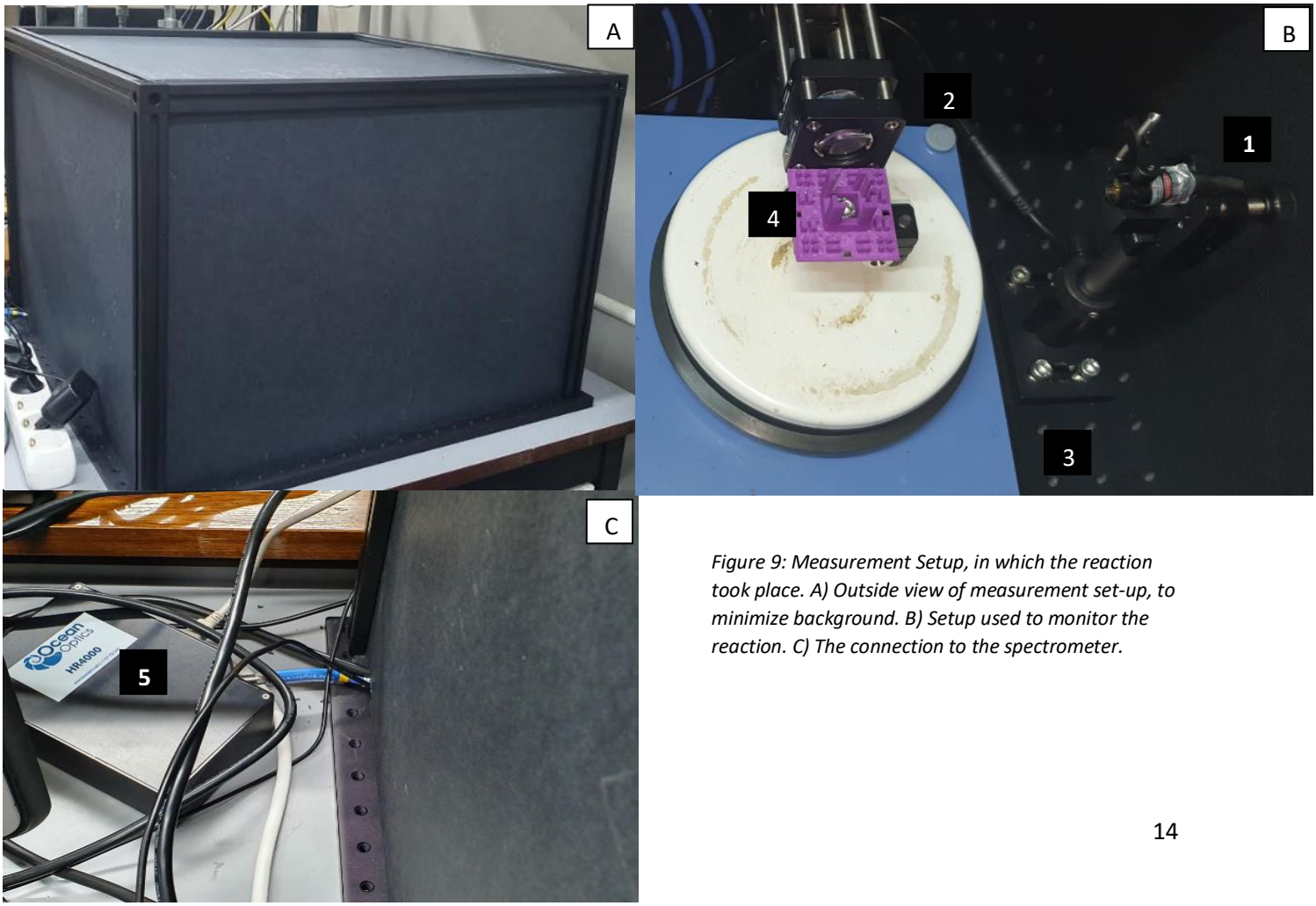

Figure 9: Measurement Setup, in which the reaction took place. A) Outside view of measurement set-up, to minimize background. B) Setup used to monitor the reaction. C) The connection to the spectrometer.

The function of different components are:

- 1: 520nm Laser, excitement of Bodipy-DMS, light source.
- 2: Lens, guides emitted light of sample to spectrometer.
- 3: Heating Plate, facilitates stirring of the sample.
- 4: Cuvet placement.
- 5: Spectrometer, Ocean Optics HR4000.

The sample preparation for measurements:

As figure 1 shows, for hydrogenation to occur, several components are needed. The hydrogen donor could be retrieved from a glove box and Bodipy-DMS was pre-synthesized by the supervisor. The catalysts were synthesized by the procedures described in the previous paragraph. The reaction was performed in a cuvet, which was filled with a volume of 1.25mL (catalyst included, added afterwards). During this research, concentrations of triethylsilane and reactant were varied. Therefore, the amount added of each chemical in a cuvet is different. In the appendix, tables are shown with the amounts of reactants added for every measurement. In every cuvet, a small stirring bar was added.

Once the reaction mixture was ready, the laser was turned on. The software used to monitor the intensity of the fluorescence over time, was set up and ready for use. The hydrogenation reaction was started by injecting Pd-nanoparticles. The program was stopped once the fluorescence intensity was constant.

Details of Spectrasuite:

Spectrasuite is software that can capture data from light sources, in this case the fluorescence intensity from the reactants. The spectra obtained are dependent on the settings chosen in the Spectrasuite software. Every measurements is done under these specific settings:

- Integration time 75 milliseconds.
- Scans per average 5.
- Saved spectra per 2 scans.

3: Results.

In this chapter acquired and analyzed data during experimental work of this research will be evaluated and discussed. The results are compared with theory and possible explanations are provided.

3.1 Catalyst nanoparticle synthesis.

As the first part of the research project, catalyst palladium nanoparticles were synthesized. The goal of this synthesis is to obtain differently shaped nanoparticles. The differently shaped Pd-nanoparticles will be used for the hydrogenation reaction in general, and will also be compared regarding their catalytic activity to each other.

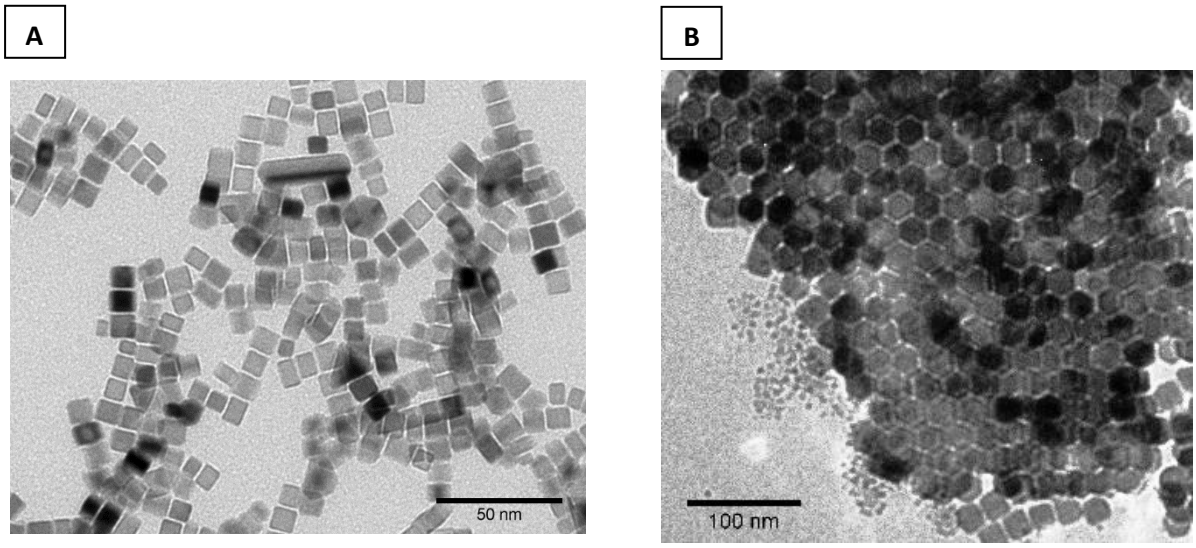

Figure 10: TEM images of Pd-Samples. Sample A is obtained by heating 11 mL of aqueous solution for 3h at 80℃, containing a mixture of Na_2PdCl_4, KBr, L-ascorbic acid and polyvinylpyrrolidone (13). Sample B is obtained by heating 11 mL of aqueous solution for 26h at 90℃, containing a mixture of Na_2PdCl_4, Sodium Citrate monobasic and polyvinylpyrrolidone (14).

The synthesis is performed by reducing a pd^{2+} salt, in the presence of polyvinylpyrrolidone, which functions as a stabilizing agent. Figure 10A shows the result of using KBR as a capping agent and L-ascorbic acid as reducing agent. Figure 10B shows that using sodium citrate as capping and reducing agent, results in different shapes. In general, different reducing agents, stabilizers and capping agents give rise to different shapes of nanoparticles (14).

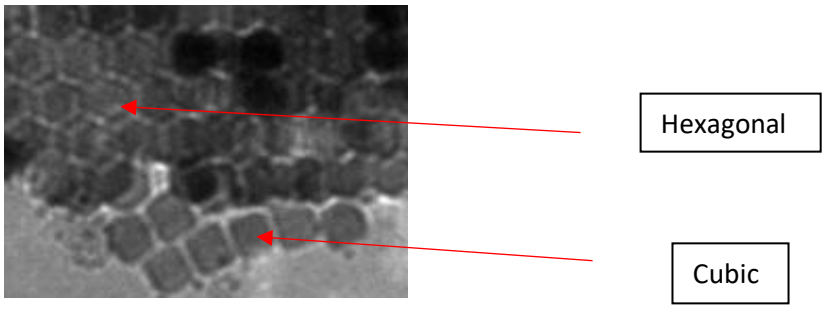

Figure 11: TEM Image of Sample 1B, zoomed in.

Secondly, the TEM image of Sample B shows multiple shapes, both hexagonal and cubic. Nevertheless, it is very unlikely that different shapes arise with the use of one specific concentration of reducing agent, stabilizer and capping agent. The different shapes appear due from which angle the nanoparticles are orientated in 2-D. Examining the image more closely, it can be assumed that the particles have adopted a cuboctahedral shape. Figure 12 shows the different faces of a cuboctahedron, and it supports the assumption that nanoparticles in Sample B adopted a cuboctahedral shape. However, Transmission Electron Microscopy might not be sufficient to verify this shape. Therefore, tomography should be carried out. Due to a lack of time, this option was neglected. If these particles have a different geometry than the assumption made, it would only have a minor impact for further concentration, catalytic activity and facet determination because they are all comparable to a spherical structure.

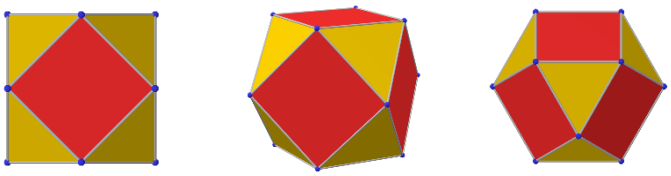

Figure 12: Colored faces of a cuboctahedron (15).

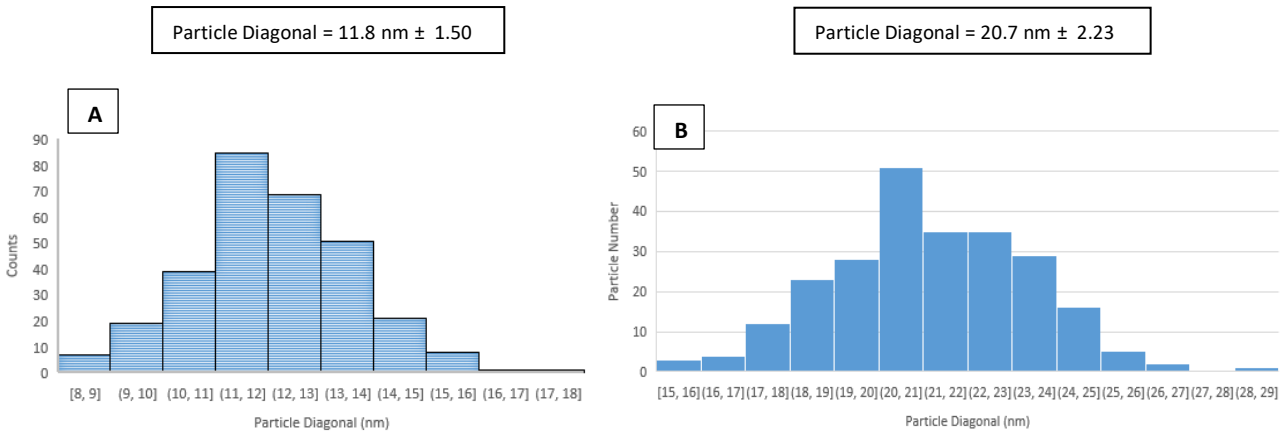

Figure 13: Particle size distributions of Sample A and Sample B, derived from TEM Images. A) Cubic Pd-nanoparticles. B) Cuboctahedron Pd-nanoparticles.

Figure 13 shows the particle size distribution of both samples, and it is clear that sample A and sample B have different sized nanoparticles. The differences in the particle size distributions have to be kept into account when eventually comparing the catalytic activity of the differently shaped nanoparticle solutions. It seems that the synthesized palladium nanoparticles are relatively monodisperse, with sample A in the variation range of 12.7% and sample B 10.8%.

At last, Inductively Coupled Plasma Atomic Emission Spectroscopy was used to determine the concentration of the Pd-nanoparticles solutions. Based on the particle size distributions, derived from the TEM-images, the volume of a single nanoparticle was determined. The volume calculation is continued by calculation on a unit cell, and finally the concentration of Pd-nanoparticles can be determined (see appendix).

3.2 Different triethylsilane concentrations.

The concentration of triethylsilane, which serves as the hydrogen donor in this particular hydrogenation reaction, is varied. The rate constants are determined for different concentrations of triethylsilane. Fluorescence spectroscopy is used to monitor the reaction. The reactant is fluorescent at 570nm, and the product is fluorescent at 520 nm.

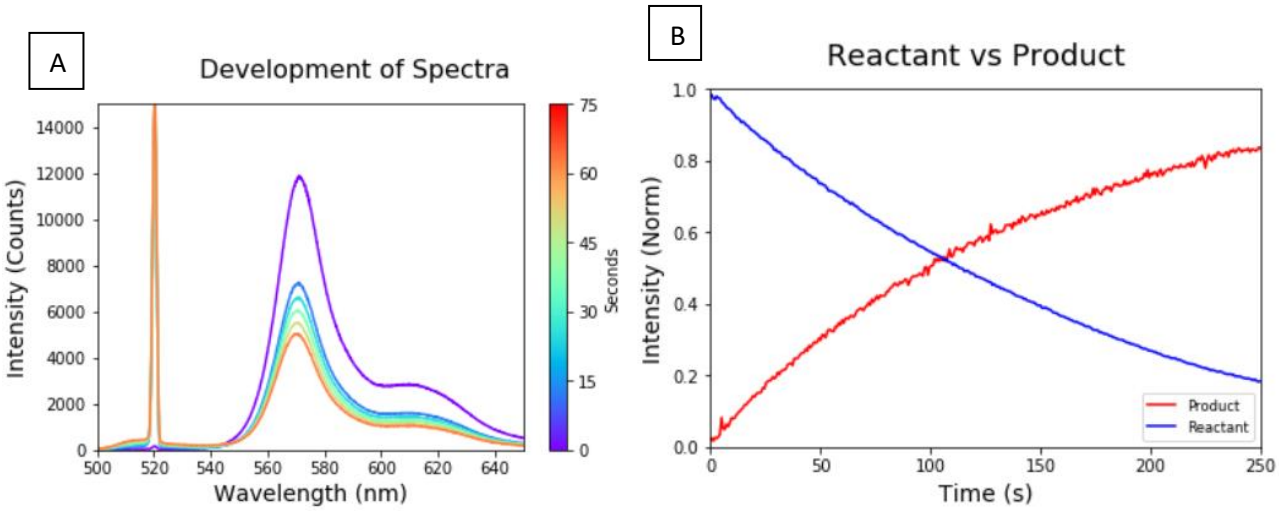

Figure 14: Overview of the data visualisation obtained from fluorescence spectroscopy. A) 5mM Triethylsilane, 1.68nm Pd-nanocubes, 3μM Bodipy-DMS. B) Normalized decrease of 570 nm for reactant, and normalized increase of product at 514 nm.

Figure 14A represents an overview of the intensity of fluorescence at different wavelengths. Intensity counts is related to the concentration of fluorescent compounds in the sample. The peak at a wavelength of 570nm represents and is related to the concentration of the reactant. On top of that, figure 14A shows a bump at approximately 600nm. This is related to the transition from the excited state in the vibrational ground state, transferred to the electronic ground state to the vibrational excited state.

Figure 14A also displays the intensity of the fluorescent peaks at 570nm over time, indicated with different colored graphs. In addition, there is an intense peak observed at 520nm. However, this peak is not related to the product formation, but associated with the scattering of the 520nm laser by Pd-nanoparticles.

Figure 14B represents a normalized graph for the decreasing reactant peak at 570 nm peak over time. The product formation is followed by monitoring the peak increase at 514 nm. The hydrogenated product is mostly fluorescent at 520nm. However the scattering of the laser caused by the catalysts, prevents any data retrieval at this particular wavelength. Because of the scattering phenomenon, it is decided that product formation will not be part of the data analysis. It is assumed that the conversion of reactant to product is 100% efficient. In addition, the product was not available in pure form. The purification of the reaction mixture was hard and a lack of time was the cause of not be able to make a calibration curve for the product.

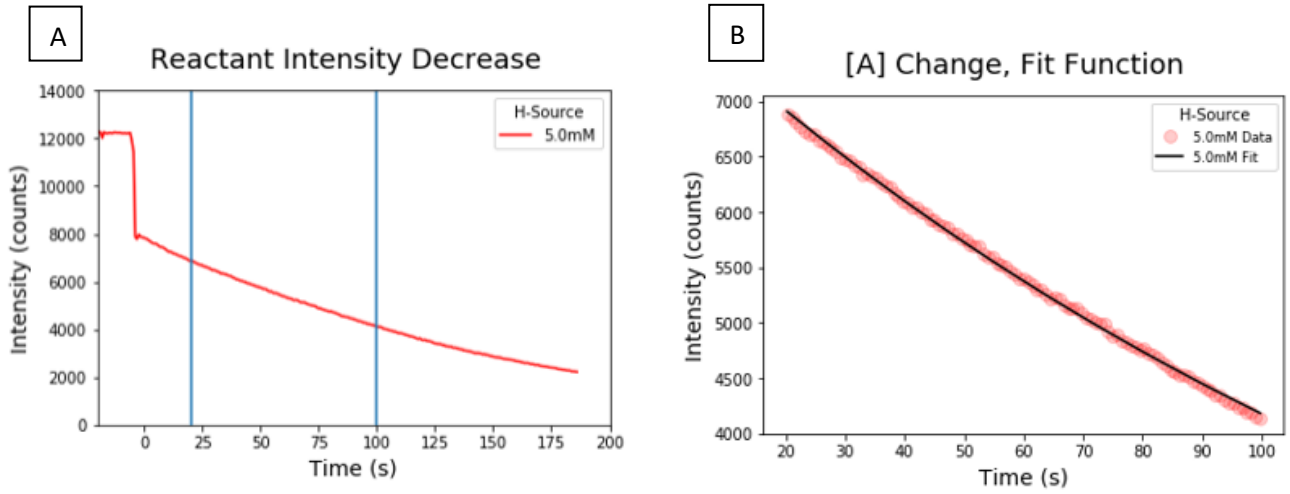

Figure 15: Reactant conversion rate for 5.0mM Triethylsilane. Catalyst Cubic Pd- Nanoparticles: 1.68nM*, Bodipy-DMS 3.0µM. A) Decrease of fluorescence peak at 570nm over time. Fit range indicated by vertical blue lines. C) Fitted theoretical function vs acquired data, determination of rate constants.*

Figure 15A shows the reactant intensity decrease over time for 5mM of triethylsilane. Multiple measurements at different concentrations of triethylsilane were performed. It must be noted that these measurements were done at least triple for every concentration. The amount of measurements for every concentration varies. This is caused by the inconsistency of the reaction. In some cases, adding Pd-nanoparticles either did not start the reaction or the fluorescence intensity decrease was very slow and quickly stabilized.

Sometimes the reactant does not fully hydrogenate, even for using 1000x excess of triethylsilane with respect to the reactant. Release of hydrogen might also play a minor role, because hydrogen could leave the reaction mixture, if not in a closed system. The ending intensities of the reactant are inconsistent as well (see appendix). The option of adding the catalytic nanoparticles through a septum does not change the inconsistency in the results. Therefore, release of hydrogen could be excluded from possible causes for the inconsistency in the results.

From figure 15A-C, the rate constant can be determined. Assumptions were made that the hydrogenation of alkenes and alkynes is pseudo first order dependent on hydrogen pressure/concentration and that the rate constant was constant throughout the reaction. With these assumptions, an exponential function (equation 17) can be fitted within the graphs to derive the rate constants for different concentrations triethylsilane.

$$[A] = [A0] * e^{-k*t} \quad [17]$$

Figure 15C shows the accuracy of the fit function and the comparison between the reactant intensity decrease and the theoretical exponential function. The fit range used varies for every concentration and is done on purpose. The range of the fit is determined by the length of exponentiality of the reactant intensity decrease function, shown by figure 15A and B. Subsequently, the rate constants can be collected from these fit functions.

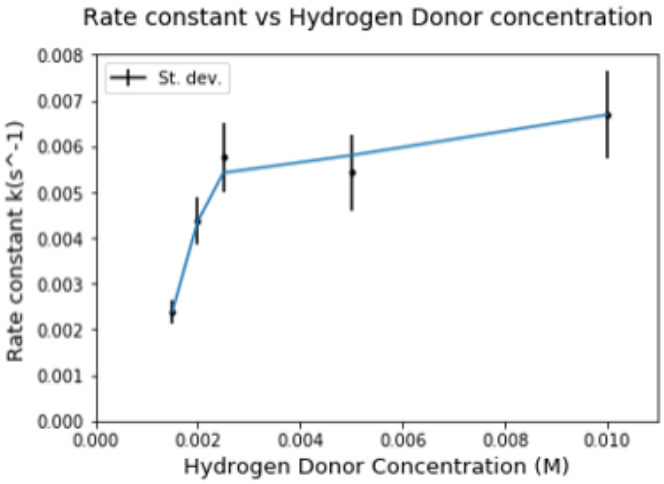

Figure 16: Rate constants vs different concentrations of triethylsilane (1.5mM, 2.0mM, 2.5mM, 5.0mM, 10mM). *Bodipy-DMS 3.0µM, Catalyst Cubic Pd-Nanoparticles: 1.68nM. Vertical lines (error bars) indicate the standard deviation of the measurements.*

Figure 16 shows an interesting trend. Firstly, the rate constants seem to be steadily increasing, up to a certain maximum, where the rate constant approximately flattens. The mechanism of hydrogenation is assumed to be following the Langmuir-Hinshelwood mechanism (8) However, this specific mechanism has a certain optimum effective reaction rate**.** Several equations were formulated before obtaining results, and based on these equations an optimum in the rate constants was expected.

The acquired experimental data, conversely, does not show any rate optimum, but it shows a maximum. One of the possible explanations is that all available active sites of the catalysts are occupied by both reactants, hydrogen and Bodipy-DMS, once the graph starts to flatten. However, this explanation can be quickly invalidated. Higher triethylsilane concentration will lead to even more competitive adsorption, which must result in a decrease of the reaction rate.

Secondly, it might be that $K_AP_A = K_BP_B$ is never true. This might be supported by the fact that we use 1000x excess of triethylsilane (1.5mM-10mM) compared to Bodipy-DMS (3μM). Therefore, an optimum may not be possible. Nonetheless, this cannot explain the increasing rate constants at the beginning. The same principle applies for this possible explanation as the previous one, more hydrogen must then lead to decreasing rate constants from the start (1.5mM).

Afterwards, a closer look is taken at the rate equation, shown by equation 16 in subchapter 2.5. During these measurements, the concentration of the hydrogen donor was approximately 1000x larger than the concentration of Bodipy-DMS. A theoretical approach is possible for the rate equation to the obtained data, shown by figure 17. This estimated (not fitted) function is relatively accurate for the obtained rate constants, and therefore it can be concluded that the hydrogenation of Bodipy-DMS is indeed following the Langmuir-Hinshelwood model. For this equation 16, several fictive values were made up, for example K_H, K_{AH} and K_A. These values were varied in order to achieve the most accurate approach function compared to the trend of the experimental data.

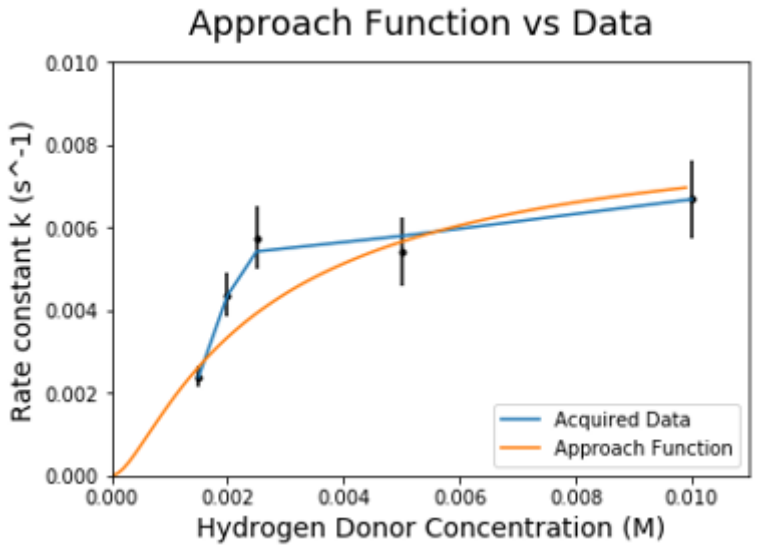

Figure 17: Theoretical approaching function vs obtained data for different concentrations of triethylsilane. Acquired data: Triethylsilane; (1.5mM, 2.0mM, 2.5mM, 5.0mM, 10mM). *Bodipy-DMS 3.0μM, Catalyst Cubic Pd-Nanoparticles: 1.68nM.*

3.3 Different Bodipy-DMS concentrations.

In the previous section, different concentrations triethylsilane and its influence on the rate constants were discussed. In theory, kinetics of this reaction are dependent on a second variable, which is the reactant concentration. Beforehand, it was assumed that the reaction was pseudo first order dependent, and therefore the concentration of Bodipy-DMS would not play a role. In this chapter, the influence of different concentrations of Bodipy-DMS, with same concentrations triethylsilane, will be discussed and evaluated.

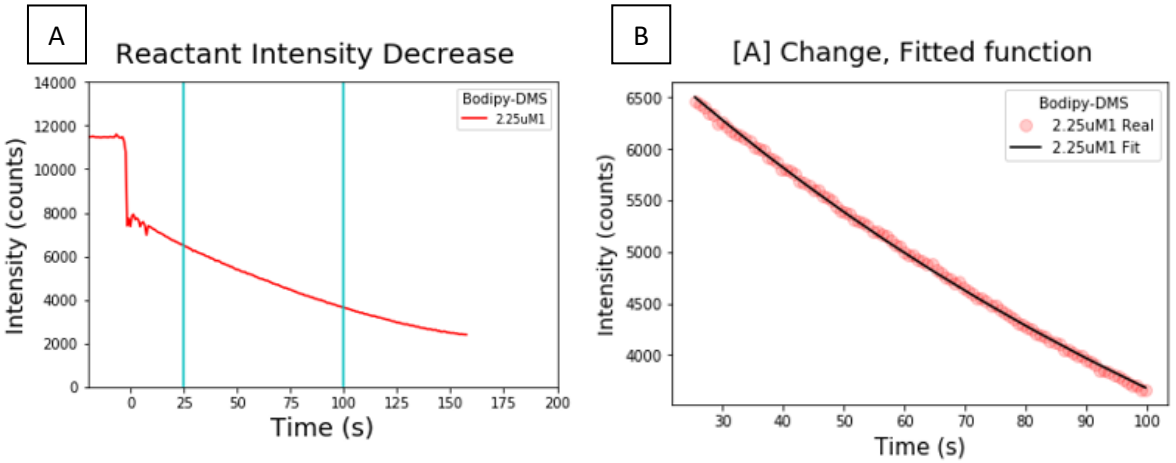

Figure 18: Reactant conversion rate for 2.25uM Bodipy-DMS. Catalyst Cubic Pd- Nanoparticles: 1.68nM. *Triethylsilane 2.5mM. A) Decrease of fluorescence peak at 570nm over time. Vertical lines indicate fit range. B) Fitted theoretical function vs acquired data, determination of rate constants.*

Figure 18A shows the reactant intensity decrease for 2.25uM of Bodipy-DMS over a given time period. As for different concentration of triethylsilane, the rate constants are determined for different concentrations Bodipy-DMS, derived from Figure 18B. These measurements are done at least tripe for every concentration as well, and equation 17 is used once more as a fit function.

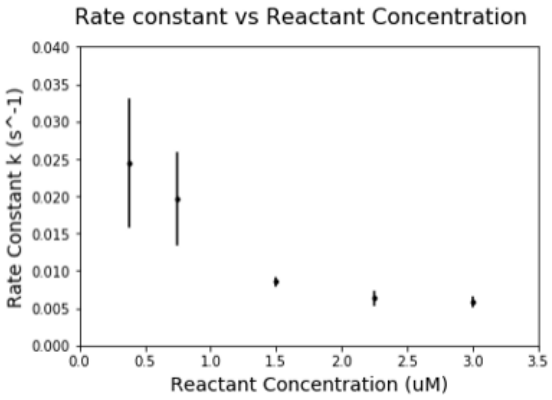

Figure 19: Rate constants for different concentrations of Bodipy-DMS (0.375µM, 0.750µM, 1.50µM, 2.25µM, 3.00µM) Catalyst Cubic Pd- Nanoparticles: 1.68nM. *Triethylsilane 2.5mM.*

An important note is that the fit range differs for every concentration (see appendix), which means that it is fitted within the exponential range of each graph. A range which is too large, might cause changes and inaccurate estimations of rate constants. The exponential fit function will not fit accurately through the data points obtained, and the determined rate constants will not be representative for the reaction. A shorter range might contain too few data points, and will not be reliable.

Figure 19 shows that with decreasing concentration of Bodipy-DMS the rate constant increases, which is an uncommon trend. In the chapter of different concentrations of triethylsilane, we saw the rate constants increasing for higher concentrations. There could be several explanations for this phenomenon. The stock solution of the reactant might be polluted with a compound that poisons the Pd-nanoparticles and decreases their catalytic activity. This would explain the inversely proportional trend of increasing rate constants for lower concentrations of reactants, which is related to the concentration of poisoning compounds.

In order to verify this assumption, one batch of Pd-Nanoparticles were treated with Bodipy-DMS stock solution beforehand, centrifuged and collected. Pd-nanoparticles that have not been treated, are centrifuged and collected.

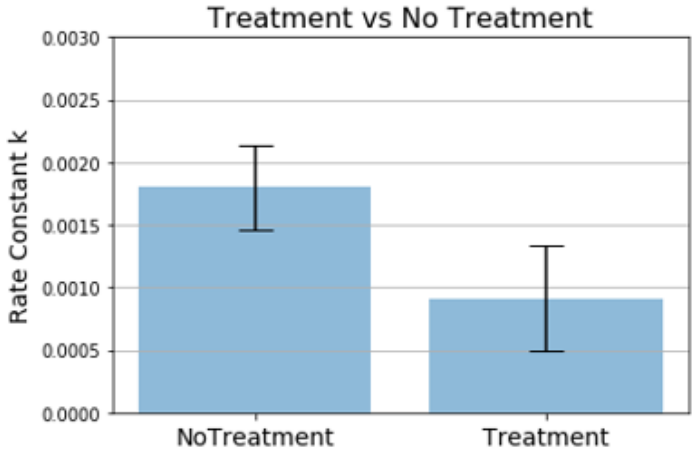

Figure 20: Rate constants for Pre-treated Pd-Nanoparticles and Untreated Pd-nanoparticles. Concentrations: Pd-Nanocubes: 1.68 nM, Bodipy-DMS 3µM, Triethylsilane 5mM.

Figure 20 shows the difference in rate constants between untreated and treated Pd-nanoparticles. It seems plausible that treatment causes a decrease in rate constants for the hydrogenation reaction. However, this method is not very accurate. With the treatment method, some supernatant was left behind, and contained an amount of Bodipy-DMS. This will cause the rate constant to decrease, according figure 19. In addition, the concentration of Pd-Nanoparticles will not be equal, and therefore hard to compare and prevent from drawing a conclusion. Finally, there are only 2 data points, and these measurements should have been performed multiple times to ensure more accurate results.

It is very plausible that the reactant stock solution contains an unknown compound or molecule, which affects the reaction. If we take a closer look at equation 16, the overall rate of the reaction, and vary the concentration of Bodipy-DMS theoretically, the rate constants will not change for these concentrations. This assumption is supported by the fact that we could plot an exponential function over a time scale of approximately 60-80 seconds for different concentrations of hydrogen donor, and the fit suited well.

3.4 Geometry dependent catalytic activity.

It is known that different geometry and differently sized catalysts/nanoparticles exhibit distinct catalytic activity (3). As addressed before, the nanoparticles have been synthesized for these experiments to investigate the difference in conversion rate/rate constants.

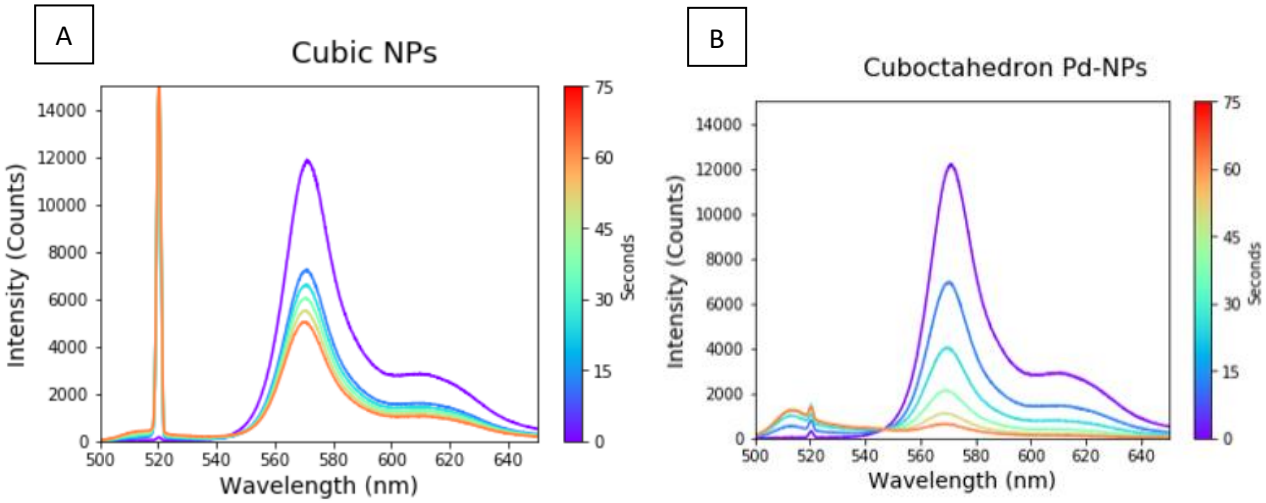

Figure 21: Spectra development over time after injection of Catalysts. A) Cubic Pd-Nanoparticles (1.68nM), B) Cuboctahedron Pd-Nanoparticles (0.106nM).

Table 3: Amount of Pd-atoms

	Concentration Pd-NP	**Amount NPs/1.25mL**	**Amount of UC**	**Amount of Pd-Atoms**
Cuboctahedron Pd-NP	1.68nM	$1.27*10^{12}$	$1.24*10^{16}$	$4.97*10^{16}$
Cubic Pd-NP	0.106nM	$6.35*10^{10}$	$5,46*10^{15}$	$2.18*10^{16}$

Table 3 shows the concentration of Pd-Atoms within the cuvet during the reaction. The difference in concentration of the Pd-atoms between both samples is more than 2 times. However, Figure 21A shows an immense peak at 520nm, which Figure 21B does not. This extreme peak at 520nm represent the scattering of the laser by the Pd-catalysts. It appears that cubic Pd-Nanoparticles scatter light more intensively.

This may be caused by Rayleigh scattering, and its intensity is dependent on d^6. Rayleigh scattering is defined as scattering of light by particles smaller sized than wavelength. The only other difference in values between both separately shaped nanoparticles is the diameter. According to Figure 10A and 10B, the TEM-images of the two samples, the cubic shaped nanoparticles seem to cluster. This can be confirmed by experimental observations. During centrifugation, the cubic Pd-nanoparticles precipitated within 30 minutes. On the contrary, cuboctahedron Pd-nanoparticles needed a centrifugation time of approximately 17 hours to partly precipitate. Clustered nanoparticles precipitate more easily than non-clustered nanoparticles. These clustered nanoparticles can be considered to be one single particle, which relates to higher particles diameters. Clustering may result in declining catalytic activity, because less surface area is available for binding molecules. However, this can not be evualated and compared fairly, because none-clustered cubic Pd-Nanoparticles have not been synthesized.

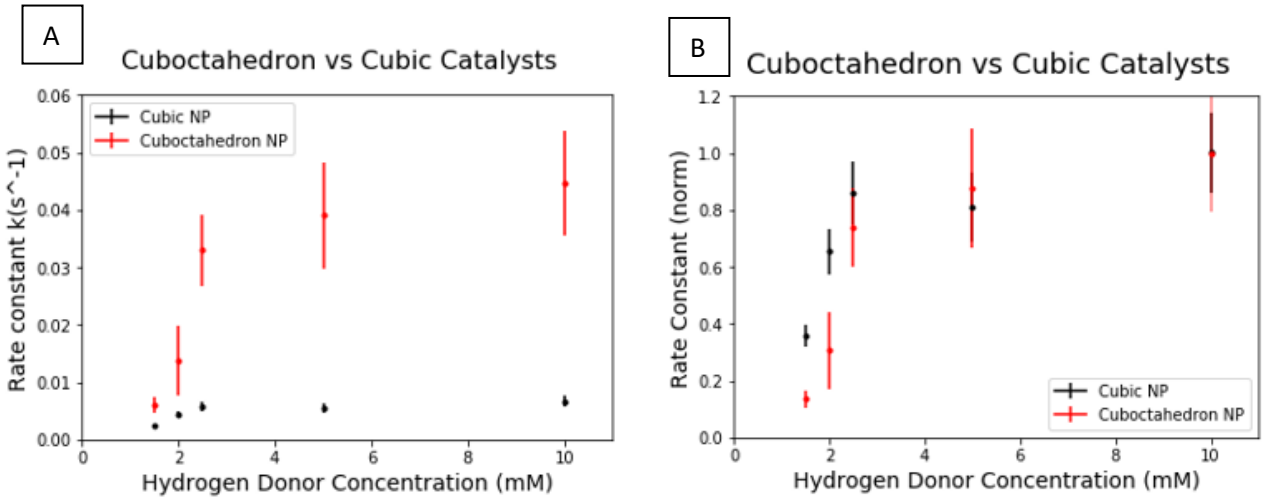

Figure 22: Rate constant for differently shaped and sized catalysts at different triethylsilane concentrations. A) Rate constants vs TES Concentrations. B) Normalized Rate Constant vs TES Concentrations.

Figure 22 indicates that cuboctahedral Pd-nanoparticles follow the same trend of rate constants for different concentrations of triethylsilane as for cubic NPs (earlier discussed in section 3.2). In addition, figure 21 clearly presents that cuboctahedron Pd-Nanoparticles express better catalytic activity than cubic Pd-Nanoparticles. One of the major differences related to different shapes, is the enclosement of the facets. As addressed before, assuming that cuboctahedron nanoparticles are enclosed by {111} and {100} facets, and cubic nanoparticles by {100} facets only. Hydrogen uptake and desorption is regulated by facets and vertices (edges of the nanoparticles) (16) . Subsequently, according to (17),(18), facets indeed play a major role regarding catalytic activity. Based from information provided by literature, we can conclude that the dissociation energy/diffusional energy on {111} facets is more positive than for {100} facets, and the activation barrier for desorption is more negative for hydrogen on {111} facets. This provide more stabilization on the catalytic surface. Therefore, cuboctahedron cause an increase of nearly 10 times associated with the rate of the reaction, even at lower concentrations compared to cubic nanoparticles.

Secondly, based on the TEM-images acquired, you can observe little clusters in the Pd-cuboctahedron sample. These will affect the rate constant, because these Pd-clusters show great activity. This may explain the difference in catalytic activity, but there are other factors (geometry), which also have to be taken into consideration.

Thirdly, the Langmuir-Hinshelwood model is carried out on the surface of the nanoparticles. Therefore, the surface must indeed be taken into account precisely in order to able to compare the catalytic activity of the differently shaped nanoparticles. Equation 18-19 are related to cubic shaped nanoparticles, and equation 20-21 are applicable to cuboctahedral shape.

Cube: $Vcube = r^3$ [18]

Cube: $Acube = 6 * r^2$ [19]

Cuboctahedron: $A = \left(6 + 2\sqrt{3}\right)a^2$ [20] (19)

Cuboctahedron: $V = \frac{5}{3}\left(\sqrt{2}\right)a^3$[21] (19)

In which r is defined as the length of the sides of a cube. For the cuboctahedron formulas, variable 'a' is defined as the length of the side of a cuboctahedron. The distance from side to side of a cuboctahedron has been measured in the TEM image, which is defined as "D". "D" can be expressed as "a" with geometry:

$$a = \frac{d}{2 * \sin(60)} [22]$$

By expressing the rate constant in terms of total surface area, the relative catalytic activity is showed with more accuracy. Surface area can be calculated based on the particle size distribution and the concentration of the Pd-nanoparticles in the reaction sample.

Table 4: Total surface area of catalysts in samples.

	Concentration (nM)	**Surface Area Single NP (nm^2)**	**Total surface area (all NP) (m^2)**
Cubic Pd-NPs	1.68	413.34	0.417
Cuboctahedral Pd-NPs	0.106	1350.7	0.0862

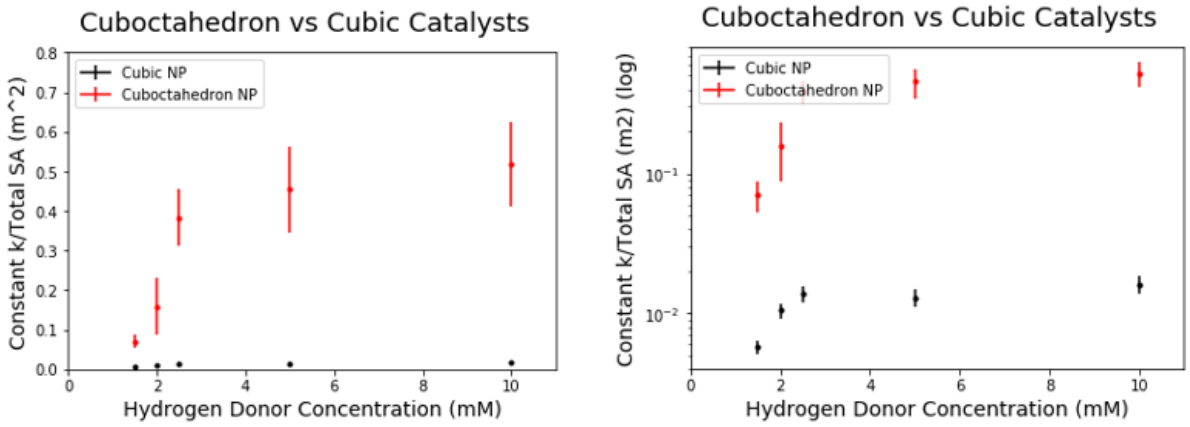

Figure 23: Rate constants for shaped nanoparticles, divided by total surface area. A) Linear scale. B) Logarithmic scale.

Figure 23 shows the rate constants divided by the total surface area, different for both catalysts. Cuboctahedron nanoparticles' rate constants reach a value of almost 0.6. On the contrary, rate constants of cubic nanoparticles hardly reach a value of 0.02. It is shown that cuboctahedron achieve 30-40x times higher catalytic activity than cubic nanoparticles. To what extend the little Pd-clusters contribute to this difference, is not clear and hard to determine. In order to evaluate the contribution of these clusters, non-clustered Pd-nanoparticles should be synthesized.

4: Conclusion

The goal of this particular research is gaining more insight in the Bodipy hydrogenation reaction, which involves both kinetics and the mechanism. The rate constants have been determined for different reaction parameters. More research can be carried out in the area of determining the particular equilibrium constants for the Langmuir-Hinshelwood mechanism. In addition, other environmental parameters could be investigated, such as pressure and temperature.

Increasing concentrations of triethylsilane, which serves as a hydrogen donor, lead to a continuous increase of rate constants. Comparing these obtained results with the rate/kinetic values associated with the Langmuir-Hinshelwood mechanism we can conclude that Pd-catalyzed hydrogenation of Bodipy-DMS follows the Langmuir-Hinshelwood mechanism.

The increase of Bodipy-DMS concentration led to an interesting discovery. The rate constants decreased with an increase of Bodipy-DMS concentrations. It is most likely that this solution contains an inhibitor, which affects the reaction at low and high concentrations. The reaction order is of Bodipy-DMS therefore -1. The stock solution should be investigated further for possible reaction inhibiting compounds.

Finally, the influence of differently shaped Pd-nanoparticle catalysts was investigated. Pd-catalysts shaped octahedral and enclosed by {111} showed higher catalytic activity than Pd-Nanocubes enclosed by {100}. The dissociation energy on {111} facets is higher than for {100}, and the desorption energy is lower for hydrogen on {111} facets. This provides more stabilization of molecules on the catalytic surface. The effect clustering on the catalytic activity of Pd-nanocubes can be further investigated by the synthesis of non-clustered Pd-nanocubes.

5: Acknowledgements

Over the past ten weeks, I have been part of the Soft Condensed Matter and Inorganic Chemistry and Catalysis department. It was very pleasant to be part of these groups, especially Soft Condensed Matter, in which I dedicated most of my time.

Secondly, but not least, I want to thank my daily supervisor Stijn Hinterding. I am very thankful for your help, guidance and patience throughout the project. You made this research project a lot more exciting and supported me when I was struggling. A special thanks to Kristel Jagtenberg is justified, for building an amazing experimental setup, so I was able to acquire data and perform measurements with ease. In addition, you were very helpful for many questions, but especially python related questions. At last, I want to thank Dr. Freddy Rabouw. The weekly meetings were helpful, and provided more insight and new ideas for my research project. Besides that, I would like to thank every member of the bravelingen meetings.

I wish group member of these departments success for the completion of their research projects!

6: Literature:

1: Santen, R. van. (2012). Catalysis in perspective: Historic review. Catalysis: From Principles to Applications, 3–19. https://doi.org/978-3-527-32349-4

2: Kitzing, S., Trin, T., & Pathare, V. (n.d.). Getting most value from your Petrochemical Catalysts. 2–3.

3: Roldan Cuenya, B., & Behafarid, F. (2015). Nanocatalysis: Size- and shape-dependent chemisorption and catalytic reactivity. Surface Science Reports, 70(2), 135–187. https://doi.org/10.1016/j.surfrep.2015.01.001

4: C. Gooijer. (2000). An Introduction to fluorescence spectroscopy. Analytica Chimica Acta, 419(1), 116–117. https://doi.org/10.1016/S0026-265X(00)00048-5

5: Klein. D.R. ed. Organic Chemistry 2nd ed. Wiley, 2013.

6: Robertson (2002) J. Diamond-like amorphous carbon. Materials Science and Engineering: R: Reports, 37(6), 129-281. https://doi.org/10.1016/S0927-796X(02)00005-0

7: Mirza-Aghayan, M., Boukherroub, R., & Bolourtchian, M. (2006). A mild and efficient palladium-triethylsilane system for reduction of olefins and carbon-carbon double bond isomerization. Applied Organometallic Chemistry, 20(3), 214–219. https://doi.org/10.1002/aoc.1036

8: Spahn. W. (2002), Transfer Hydrogenation: Emergence of the Metal-Ligand Bifunctional Mechanism, 45-48.

9: Mattson, B., Foster, W., Greimann, J., Hoette, T., Le, N., Mirich, A., … Schwanke, E. (2013). Heterogeneous catalysis: The horiuti-polanyi mechanism and alkene hydrogenation. Journal of Chemical Education, 90(5), 613–619. https://doi.org/10.1021/ed300437k

10: Rothenberg, G., Catalysis, Concepts and Green Applications 2nd ed. Wiley, 2017.

11: University of Illinois, Introduction to Surface Reactions. Accessed on 19-06-2019

12: https://biocyclopedia.com/index/chem_lab_methods/heating.php

13: Kim, S. K., Kim, C., Lee, J. H., Kim, J., Lee, H., & Moon, S. H. (2013). Performance of shape-controlled Pd nanoparticles in the selective hydrogenation of acetylene. Journal of Catalysis, 306, 146–154. https://doi.org/10.1016/j.jcat.2013.06.018

14: Lim, B., Jiang, M., Tao, J., Camargo, P. H. C., Zhu, Y., & Xia, Y. (2009). Shape-controlled synthesis of Pd nanocrystals in aqueous solutions. Advanced Functional Materials, 19(2), 189–200. https://doi.org/10.1002/adfm.200801439

15: P. Tilman, Own Work, Wikipedia, Accessed 19-06-2019.

16: Johnson, N. J. J., Lam, B., MacLeod, B. P., Sherbo, R. S., Moreno-Gonzalez, M., Fork, D. K., & Berlinguette, C. P. (2019). Facets and vertices regulate hydrogen uptake and release in palladium nanocrystals. Nature Materials, 18(5), 454–458. https://doi.org/10.1038/s41563-019-0308-5

17: Benkhaled, M., Descorme, C., Duprez, D., Morin, S., Thomazeau, C., & Uzio, D. (2008). Study of hydrogen surface mobility and hydrogenation reactions over alumina-supported palladium catalysts. Applied Catalysis A: General, 346(1–2), 36–43. https://doi.org/10.1016/j.apcata.2008.04.043

18: Kim, S., Lee, D. W., & Lee, K. Y. (2014). Shape-dependent catalytic activity of palladium nanoparticles for the direct synthesis of hydrogen peroxide from hydrogen and oxygen. Journal of Molecular Catalysis A: Chemical, 391(1), 48–54. https://doi.org/10.1016/j.molcata.2014.03.026

19: http://mathworld.wolfram.com/Cuboctahedron.html. Accessed on 21-06-2019.

7: Appendix

7.1: Different concentrations of triethylsilane.

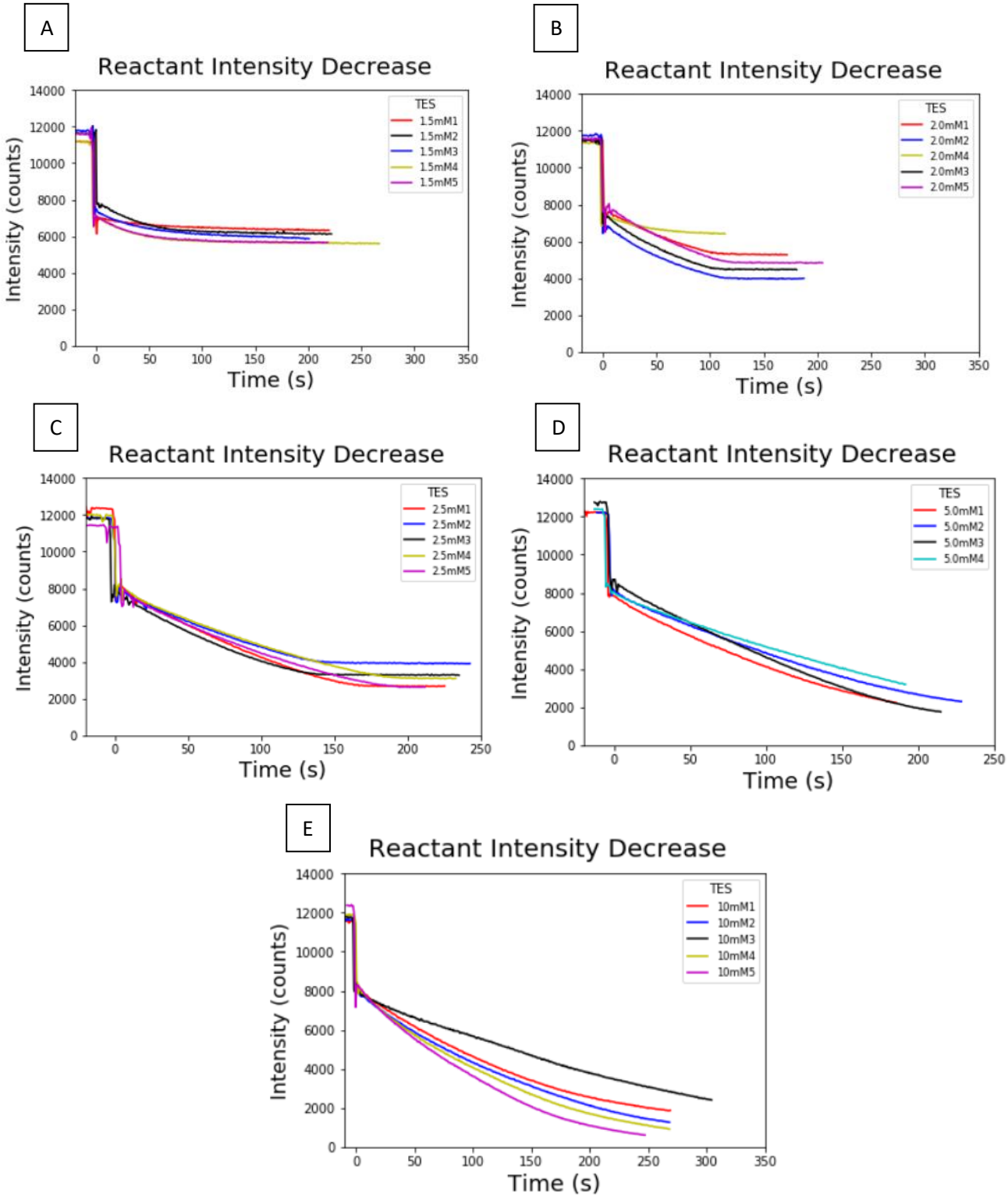

Figure 24: Decrease of reactant peak over time for different concentrations of triethylsilane. A) 1.5mM, B) 2.0mM, C) 2.5mM, D) 5.0mM, E) 10mM. Bodipy-DMS 3µM, Pd-nanocubes 1.68nM.

Fitted functions:

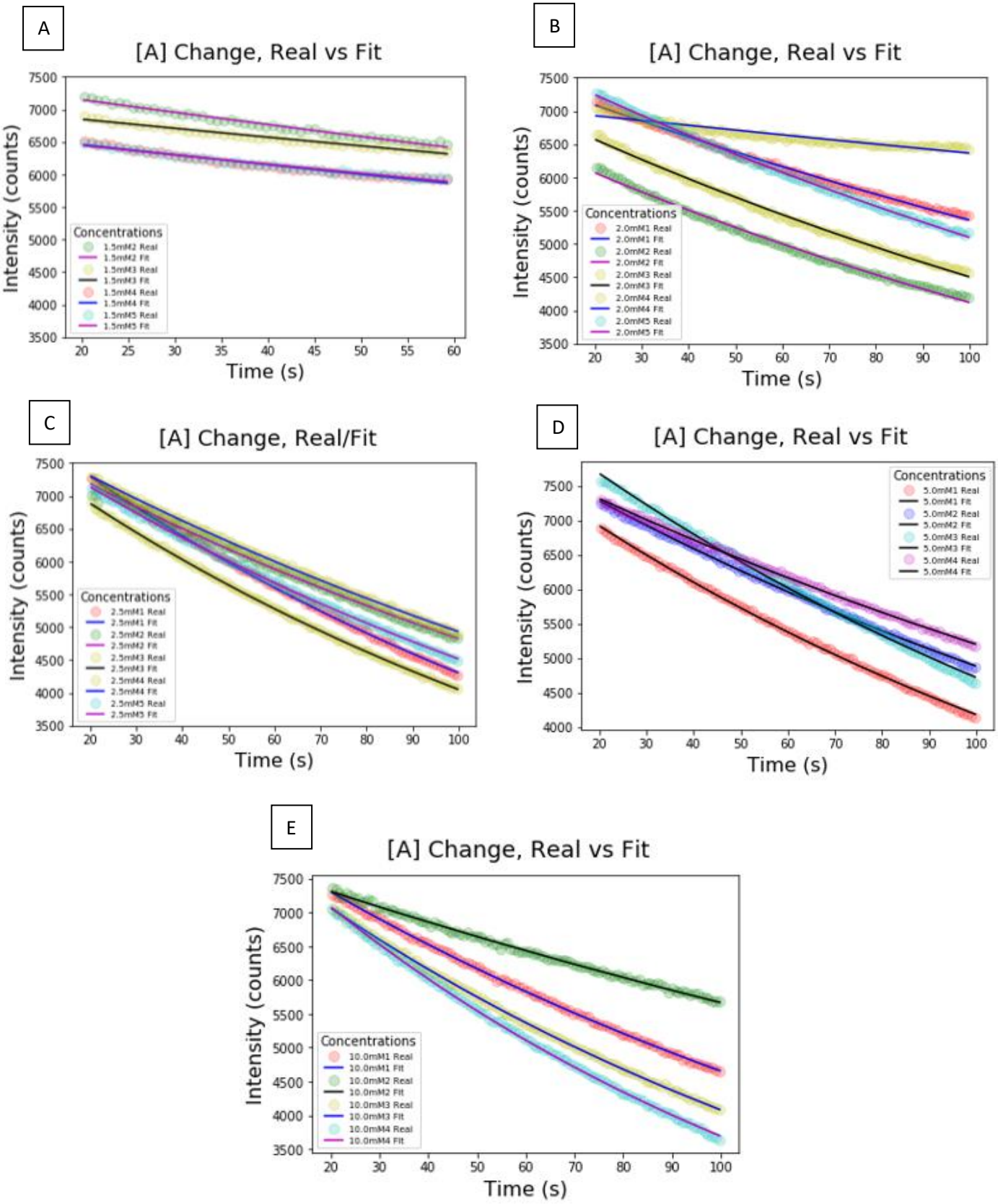

Figure 25: Fitted theoretical function vs acquired data for different concentrations of triethylsilane. A) 1.5mM, B) 2.0mM, C) 2.5mM, D) 5.0mM, E) 10mM. Bodipy-DMS 3µM, Pd-nanocubes 1.68nM.

7.2: Different Bodipy-DMS concentrations.

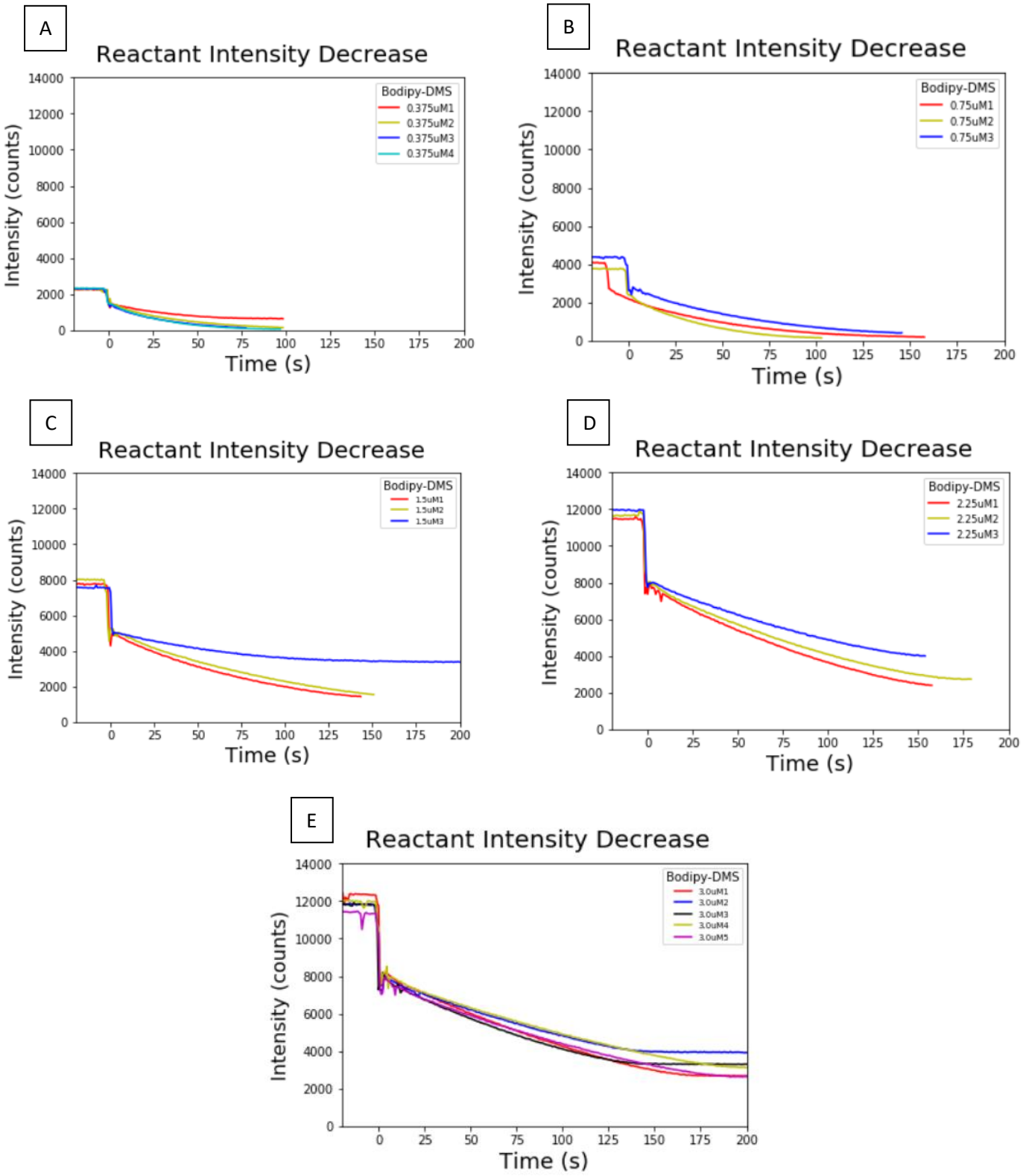

Figure 26: Decrease of reactant peak over time for different concentrations of Bodipy-DMS. A) 0.375 µM, B) 0.750 µM, C) 1.50 µM, D) 2.25 µM, E) 3.00 µM. Triethylsilane 2.5mM, Pd-nanocubes 1.68nM.

Fitted functions.

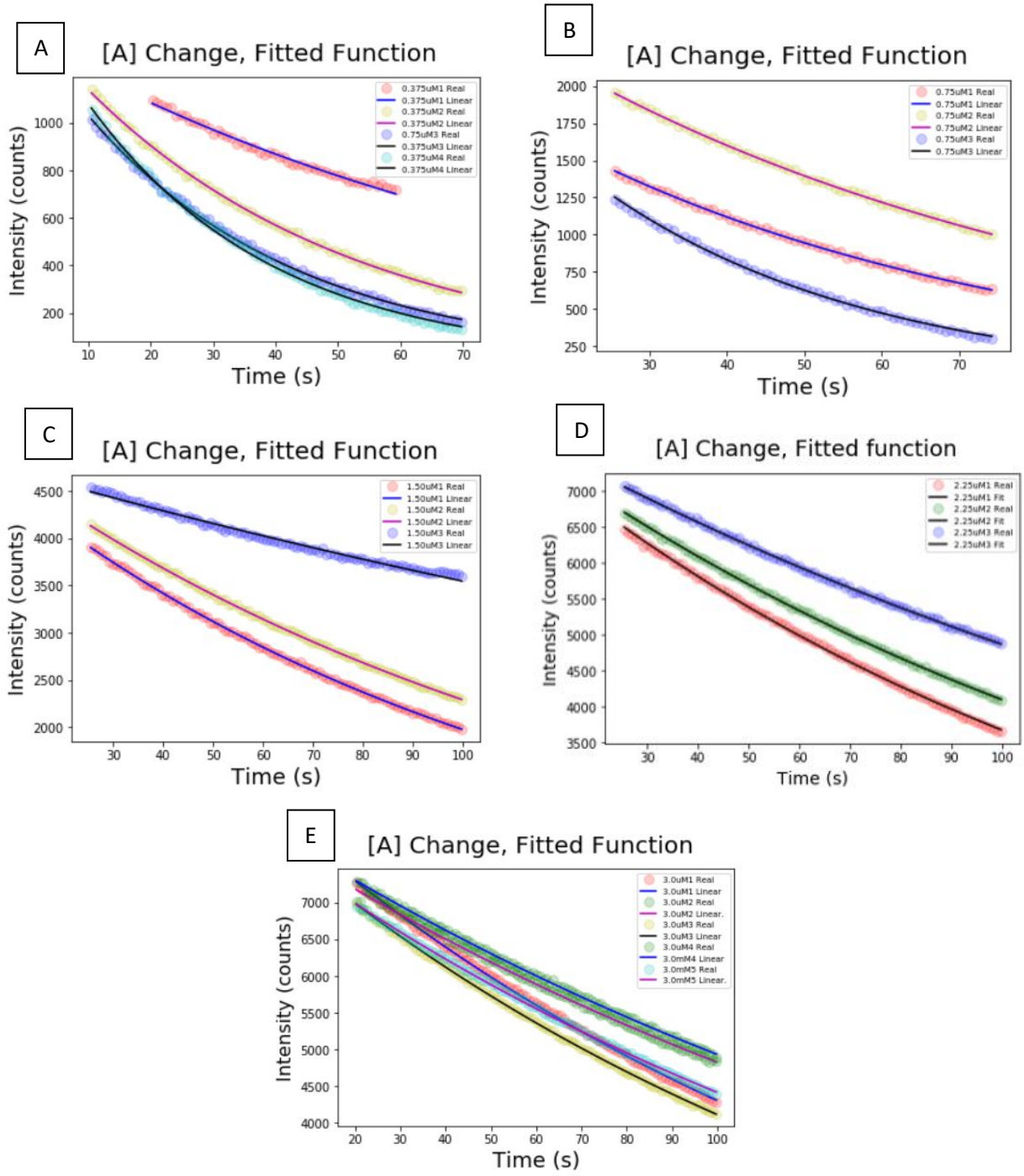

Figure 27: Fitted theoretical function for different concentrations of Bodipy-DMS. A) 0.375 µM, B) 0.750 µM, C) 1.50 µM, D) 2.25 µM, E) 3.00 µM. Triethylsilane 2.5mM, Pd-nanocubes 1.68nM.

7.3: Cuboctahedron Pd-NPs.

Different concentration of triethylsilane.

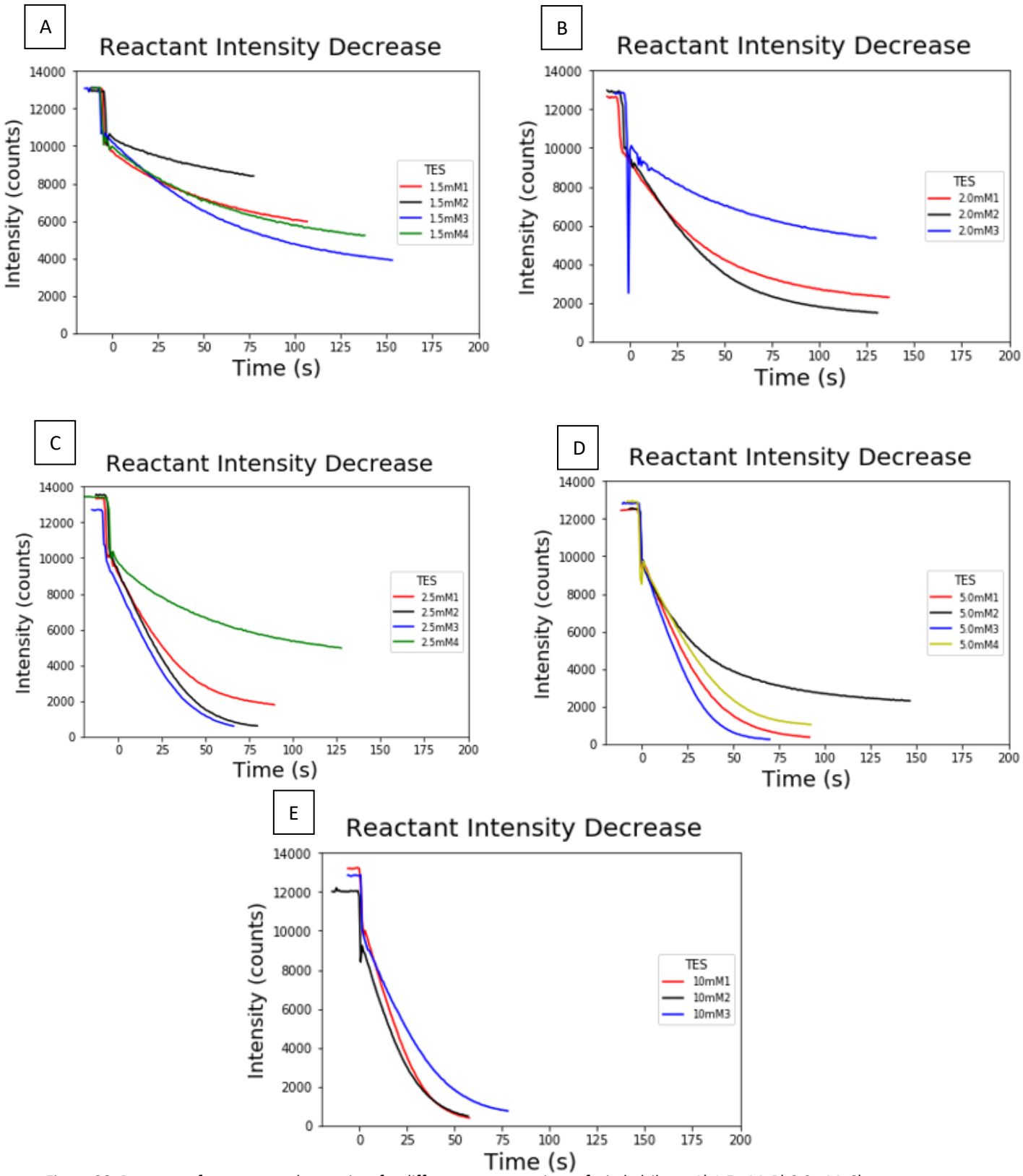

Figure 28: Decrease of reactant peak over time for different concentrations of triethylsilane. A) 1.5mM, B) 2.0mM, C) 2.5mM, D) 5.0mM, E) 10mM. Bodipy-DMS 3µM, Catalyst: Pd-cuboctahedrons 0.106nM. .

Fitting Function.

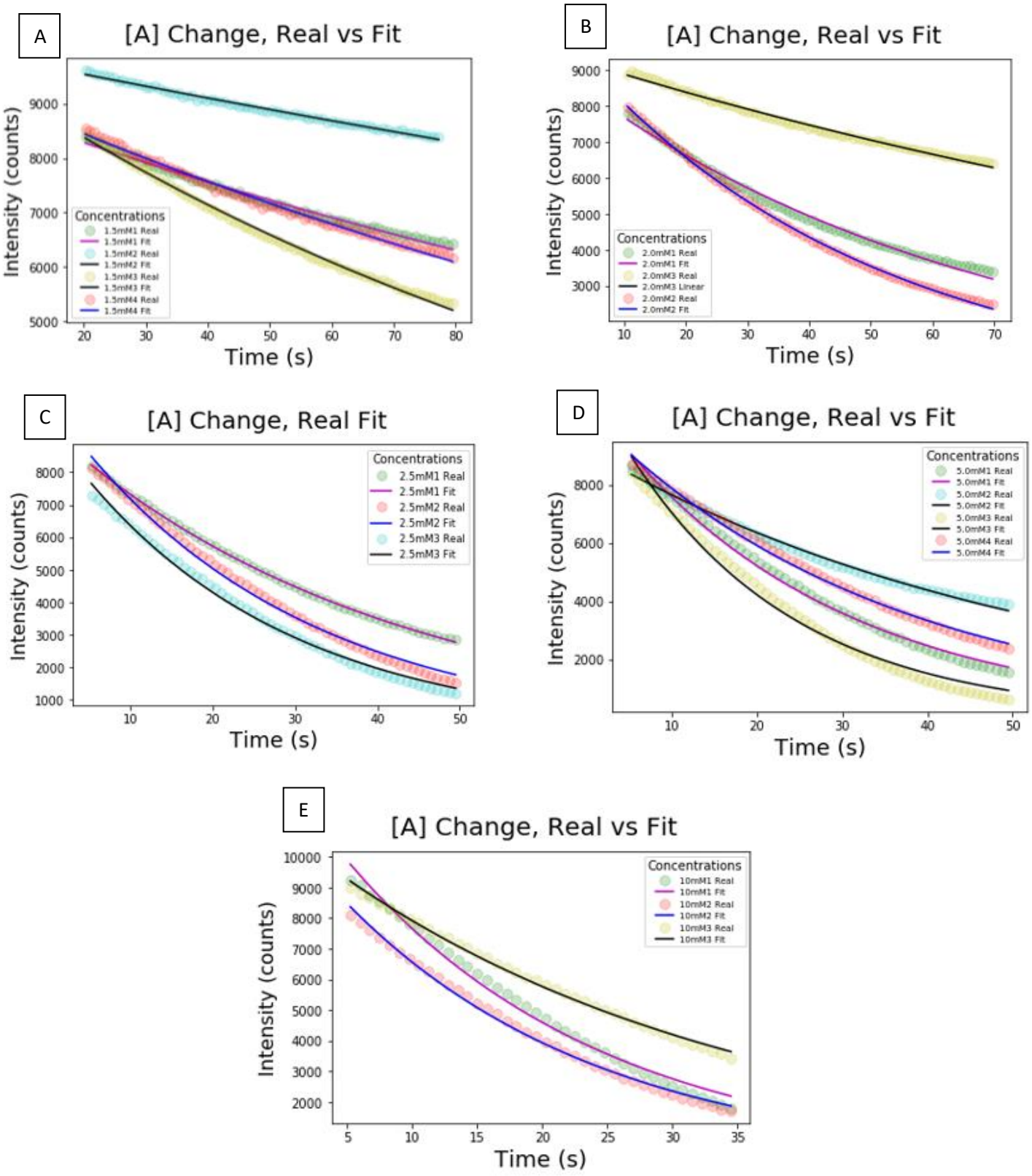

Figure 29: Fitted theoretical function vs acquired data for different concentrations of triethylsilane. A) 1.5mM, B) 2.0mM, C) 2.5mM, D) 5.0mM, E) 10mM. Bodipy-DMS 3µM, Catalyst: Pd-cuboctahedrons 0.106nM.

7.4: Pd-nanoparticle synthesis protocols.

Protocol synthesis Cubic Pd-nanoparticles (12).

1. Measure/Weigh 106 milligram Polyvinylpyrrolidone (PVP).
2. Measure/Weigh 301 milligram of KBr.
3. Measure/Weigh 60 milligram of L-ascorbic acid.
4. Dissolve all chemicals in 8 mL of water.
5. Heat the solution up to 80 °C.
6. Solve 52.9 milligram of Na_2PdCl_4 in 3 mL of water.
7. Subsequently, add 3 mL of 0.06 M Na_2PdCl_4 to the heated up solution of PVP, KBR and L-ascorbic acid.
8. Stir the mixture for 3 hours at 80°C.
9. Centrifuge the solution.
10. Disperse the precipitates in acetone. Subsequently, centrifuge the solution.
11. Wash the Pd-NPs with a mixture of ethanol and n-hexane.
12. Repeat step 11.

Protocol synthesis Octahedron Pd-nanoparticles (13).

13. Weigh 45.23 milligram Polyvinylpyrrolidone (PVP).
14. Weigh 66.2 milligram of Sodium Citrate Monobasic.
15. Dissolve all chemicals in 8 mL of water.
16. Heat the solution up to 80 °C.
17. Solve 27.93 milligram of Na_2PdCl_4 in 3.5 mL of water.
18. Subsequently, add 3 mL of Na_2PdCl_4 – solution to the heated up solution of PVP and Sodium Citrate Monobasic.
19. Stir the mixture for 26 hours at 90°C.
20. Centrifuge the solution.
21. Disperse the precipitates in acetone. Subsequently, centrifuge the solution.
22. Wash the Pd-NPs with a mixture of ethanol and n-hexane.
23. Repeat step 11.

7.5: Measurement sample preparation.

Concentrations of pure TES: 6.26M.

Concentrations of Bodipy-DMS Stock: 0.232 mM.

Table 6: TES Concentrations Pd-Cubic Nanoparticles.

Sample	Amount TES (400x diluted)	Amount Bodipy (10x diluted)	Amount EtOH	Amount Cubic Catalyst (4x diluted)
1	120 µL	160 µL	770 µL	200 µL
2	160 µL	160 µL	730 µL	200 µL
3	200 µL	160 µL	690 µL	200 µL
4	400 µL	160 µL	490 µL	200 µL
5	800 µL	160 µL	90 µL	200 µL

Table 7: TES Concentrations Pd-Cuboctahedron Nanoparticles.

Sample	Amount TES (400x diluted)	Amount Bodipy (10x diluted)	Amount EtOH	Amount Cubic Catalyst (10x diluted)
1	120 µL	160 µL	770 µL	200 µL
2	160 µL	160 µL	730 µL	200 µL
3	200 µL	160 µL	690 µL	200 µL
4	400 µL	160 µL	490 µL	200 µL
5	200 µL(100x dil.)	160 µL	690 µL	200 µL

Table 8: Reactant Concentrations.

Sample	Amount TES (400x diluted)	Amount Bodipy (10x diluted)	Amount EtOH	Amount Cubic Catalyst (4x diluted)
1	200 µL	20 µL	830 µL	200 µL
2	200 µL	40 µL	810 µL	200 µL
3	200 µL	80 µL	770 µL	200 µL
4	200 µL	120 µL	730 µL	200 µL
5	200 µL	160 µL	690 µL	200 µL

7.6: ICP sample preparation:

Estimations are based on Pd-salt added and yield

- Estimated concentration Cubic: 0.646 mg/mL Pd (100% yield)
- Estimated concentration Cuboctahedron: 0.598 mg/mL (50% yield)

Table 9: ICP sample preparation.

Sample	Amount Pd-solution	Mg Palladium	Concentration
Cuboctahedron	100 µL	0.059mg	12 ppm
Cuboctahedron	20 µL	0.0012mg	2.4 ppm
100x diluted Cuboctahedron	100 µL	$5.95*10^{-4}$ mg	0.12 ppm
Cubic	100 µL	0.0646 mg	13 ppm
Cubic	10 µL	0.00646 mg	1.3 ppm
100x diluted Cubic	100µL	0.000646mg	0.13 ppm

7.7: Pd-nanoparticle solution concentration calculations.

	Mg/L	Weight Before	Weight After Addition	Weight of Volume	Total Volume
Pd-Cubic-0.13ppm	0,042	6,7465	11,888	5,1415	5,15
Pd-Cubic-1.3ppm	0,303	6,7226	11,9375	5,2149	5,23
Pd-Cubic-13ppm	2,665	6,7458	11,9806	5,2348	5,25
Pd-Octahedron-0.12ppm	0,053	6,741	11,8834	5,1424	5,15
Pd-Octahedron-1.2ppm	0,396	6,8532	11,934	5,0808	5,09
Pd-Octahedron-12ppm	3,572	6,7645	11,8788	5,1143	5,12

Figure 29: Weight of Vials for ICP Samples.

CUBIC:				Mg/Total Volume	Mg/mL Pure Sample	
Mass Pd atom (g):	1,76719E-22		Pd-Cubic-0.13ppm	0,000216376	0,216375752	100x verdund 100 uL
Mass FCC unit cell (g):	7,06875E-22		Pd-Cubic-1.3ppm	0,001583281	0,158328126	100x verdund 1 mL
Edge length Nanoparticle in nm:	8,3		Pd-Cubic-13ppm	0,013978699	0,139786994	100 uL Pure
Volume of Nanoparticle in nm^3:	571,787		Pd-Octahedron-0.12ppm	0,000273093	0,273093387	100x verdund 100 uL
Edge length of Unit cell in nm:	0,388		Pd-Octahedron-1.2ppm	0,002016029	0,201602886	100x verdund 1mL
Volume Unit Cell in nm^3	0,058411072		Pd-Octahedron-12ppm	0,018304889	0,183048894	100 uL Pure
Volume Unit Cell in cm^3	5,84111E-23					
Density Unit Cell(g/cm^3):	12,10172606		**CUBIC**			**Cuboctahedron/Sphere**
Amount Unit Cells in NP:	9789,017397		Gemiddelde Pd-Cubic (g)/mL	**0,000171497**	Gemiddelde Pd-Cuboctahedron (g/mL)	**0,000192326**
			Aantal Pd(C)Unit Cells/mL:	2,42613E+17	Aantal Pd(C)Unit Cells/mL:	2,72079E+17
Octahedron:			Aantal Pd(C) Atoms/mL:	9,70452E+17	Aantal Pd(C) Atoms/mL:	1,08832E+18
Mass Pd atom (g):	1,76719E-22		Aantal NPs/mL	2,47842E+13	Aantal NPs/mL	3,95459E+12
Mass FCC unit cell (g):	7,06875E-22		Aantal NPs/L	2,47842E+16	Aantal NPs/L	3,95459E+15
Diameter of Nanoparticles in nm:	20,692		Aantal NPS in molair	4,11561E-08	Aantal NPS in molair	6,5669E-09
Amount Unit Cells in NP:	6,88E+04			41nM		6,6nM
Volume of Nanoparticle in nm^3:	4018,734129					
Volume Unit Cell in nm^3	0.058411072					

Figure 30: Calculations of Pd-NPs concentrations within stock solution.

	Yield (%)	68,79317055	Yield (%)
Concentration Measure	1,68nM (Cubic)	0,106nM (Cubocta)	
Amount NPs/mL	1,01555E+12	63513068249	
Amount NPs/1,25mL	1,26943E+12	79391335312	
Amount of UC	1,24265E+16	5,4622E+15	
Amount of Pd-Atoms	4,97061E+16	2,18488E+16	
Surface Area NP Cubic:	413,34	Surface Area NP Cuboctahedron	1350,712999
Volume of Cubic:	571,787	Volume of Cuboctahedron:	4018,734129
	0,722891566		0,336104095

Figure 31: Calculation Yields of synthesis.